JOURNAL OF PETROLOGY | VOLUME 47 | NUMBER 11 | PAGES 2073–2104 | 2006 | doi:10.1093/petrology/egl037

Replenishment, Crystal Accumulation and Floor Aggradation in the Megacrystic Kameruka Suite, Australia

W. J. COLLINS[1]*, R. A. WIEBE[2], B. HEALY[1] AND S. W. RICHARDS[1]†

[1]DISCIPLINE OF GEOLOGY, UNIVERSITY OF NEWCASTLE, NEWCASTLE, NSW, 2308, AUSTRALIA

[2]DEPARTMENT OF EARTH AND ENVIRONMENT, FRANKLIN AND MARSHALL COLLEGE, LANCASTER, PA 17604-3003, USA

RECEIVED MARCH 15, 2004; ACCEPTED JUNE 13, 2006; ADVANCE ACCESS PUBLICATION AUGUST 2, 2006

Detailed field evidence indicates that the Kameruka Suite plutons of the Bega Batholith, eastern Australia, grew by crystal accumulation on the floor of a magma chamber. Depositional features in the plutons, including mafic enclave channels, asymmetric enclave pillows and exotic rafts, load casts and flame structures, and graded and trough cross-beds, indicate that the pluton built progressively upward. The general eastward dip of depositional features in the main pluton implies a lower western and upper eastern contact, consistent with a basal granite–migmatite contact in the west and a sharp hornfelsic sidewall contact in the east. Mafic, felsic and composite dykes, most common near and below the basal western contact, are interpreted as conduits for magma chamber replenishment and imply open-system behaviour during pluton construction. Textural relations are also consistent with an open-system, cumulate origin. Typically, centimetre-scale grains of quartz, plagioclase and megacrystic alkali feldspar form a touching framework with interstices filled with smaller biotite flakes and smaller intercumulus quartz and feldspar crystals. Alkali feldspar megacrysts vary from euhedral and unzoned, to mantled and partially replaced by plagioclase, to ovoid and completely pseudomorphed by quartz–albite aggregates. The common occurrence of mantled and pseudomorphed alkali feldspar in mafic enclaves, and in hybrid tonalitic rocks forming the matrix to enclave swarms, suggests that replacement or resorption of granitic primocrysts was associated with mafic replenishments. The occurrence of all megacryst types at outcrop scale implies extended alkali feldspar crystallization in different parts of the chamber, thorough stirring during, or after, periodic replenishment, and final settling in a cumulate mush. The bulk composition of the cumulate mush, represented by granodiorite, cannot represent the emplaced magma. Compositional variation can be modelled by variable degrees of crystal accumulation from a parental, silica-rich melt represented by the silicic dykes. As dykes periodically fed the magma chamber, crystals accumulated on the floor, and more evolved melts probably erupted from its roof. Thus, the average composition of the magma, and the cumulus minerals, may have remained relatively constant, and the sublinear chemical trends that typify the Kameruka Suite simply reflect differing proportions of melt and cumulate material. Sublinear chemical trends can also be explained by a restite model; however, the distinctive Ba, light rare earth element and Zr spikes at high silica can be explained only by a cumulate model, which also explains why the low-silica granites of the suite share the same chemical characteristics as the high-silica granites.

KEY WORDS: *crystal accumulation; magma chamber; open system; granitoids; Kameruka; Australia*

INTRODUCTION

The concept that some igneous rocks represent accumulations of early-formed crystals (i.e. cumulate rocks) was first clearly articulated by Wager & Deer (1939) in their classic study of the Skaergaard layered intrusion. Since that time, despite many questions (e.g. Campbell, 1978; McBirney & Hunter, 1995), the cumulate model has been widely applied and has successfully provided a valuable framework for understanding the origin of mafic plutonic rocks (Irvine, 1982). Although some granitic plutons have internal structures that closely resemble depositional features in mafic intrusions, these features are relatively scarce and often rather subtle.

*Corresponding author. Present address: School of Earth Sciences, James Cook University, Townsville, Qld. 4811, Australia. E-mail: bill.collins@jcu.edu.au.

†Present address: Research School of Earth Sciences, The Australian National University, Canberra, ACT 0200, Australia.

They have only rarely been interpreted as originating by crystal-sorting at a boundary between a relatively solid floor of cumulus crystals and overlying liquid (Gilbert, 1906; Emeleus, 1963; Wiebe & Collins, 1998).

The probability of crystals settling in a granitic melt has long been deemed unlikely by most petrologists for two reasons: (1) the apparently high viscosity of granitic melt was thought to prohibit any settling; (2) even if the melt were a Newtonian liquid, the low density contrast between the melt and crystals (mainly quartz and feldspar) would cause the crystals to sink too slowly (Bartlett, 1969). Some more recent experimental data lessen the strength of these arguments by showing that small amounts of water can lower the viscosity of granitic melts much more than had been previously thought (Baker, 1998). Although Stokes' Law calculations do indicate slow rates of settling for individual crystals, larger packages of crystals and interstitial melt could settle much more rapidly. Crystalline mushes (weakly attached crystals and interstitial melt) are expected to form along the margins and roof of a magma chamber during peripheral cooling (Marsh, 1988). If disrupted by external events (e.g. earthquakes, magma chamber replenishments, eruptions) these semi-coherent mushy packages would settle downward as a crystal-rich 'slurry' much more rapidly than single crystals, and form deposits on the chamber floor. Some of these settling features have already been described in granitic plutons (Wiebe & Collins, 1998), and others are documented in detail below.

Detailed field and petrographic observations, combined with chemical and isotopic constraints, are used to develop a physical model showing that the Kameruka pluton and associated Pericoe and Illawambra plutons of the Lachlan Fold Belt, southeastern Australia, were constructed by the deposition of cumulus minerals on the aggrading floor of a magma chamber that was affected by periodic replenishments of felsic and subordinate mafic magma. The model has broad implications for understanding compositional variation and pluton construction mechanisms in other granite suites.

BEGA BATHOLITH

The Bega Batholith (Fig. 1) is the largest composite intrusion in the Palaeozoic Lachlan Fold Belt of eastern Australia, extending meridionally for more than 300 km adjacent to the east coast. A comprehensive petrological and geochemical study of the Batholith (Beams, 1980) revealed over 130 plutons, which were grouped into some 50 suites, in turn grouped into seven super-suites. Although Chappell (1996*a*) defined granite suites as 'groups of plutons possessing characteristic features that are a result of their derivation from source material of specific composition', a non-genetic definition considers that they exhibit distinct field and textural features and that chemical variation shows a high degree of correlation, such that whole-rock chemical analyses fall on the same, approximately linear, trends on Harker variation diagrams. Super-suites comprise several suites that do not fall strictly on the same linear chemical trends, but have sufficient textural and chemical similarity to be grouped together. Like the Bega Batholith itself, the super-suites are aligned north–south, and some extend the entire 300 km length, although they are rarely more than 15 km wide. The marked chemical differences between super-suites leads to a striking chemical and isotopic asymmetry across the batholith, with the western units being low in Na, Sr, Al and P, whereas the eastern units are systematically higher in those elements (Beams, 1980). This chemical asymmetry appears to be reflected isotopically (Chappell *et al.*, 1991).

FIELD RELATIONS IN THE KAMERUKA, ILLAWAMBRA AND PERICOE PLUTONS

The Kameruka Suite (Fig. 1) comprises the Kameruka, Illawambra and Pericoe plutons (Chappell *et al.*, 1991), the latter two at opposite ends. The three plutons have gradational and locally complex contacts, and, thus, we suggest that they may better be considered as 'facies variants' within an elongate, possibly long-lived magma chamber, rather than as a set of separate plutons. Thus, we use the terms Illawambra and Pericoe to indicate plutons and texturally comparable phases interlayered with or gradational to the Kameruka pluton.

The ~420 Myr old Kameruka Suite is about 100 km long and reaches a maximum width of 14 km near Bega (Fig. 1). Excellent exposures within the Bega River provide a near-complete east–west traverse through the Kameruka pluton. The western contact of this pluton dips moderately to the east, subconcordant with underlying, migmatitic Ordovician metasediments and interlayered, metre-scale granitoid sheets. In contrast, the eastern contact is steep to subvertical and locally marked by sharp, cross-cutting contacts between granodiorite and hornfelsed country rock, which is not migmatitic. Scarce angular blocks of country rock, up to house size, occur near the eastern contact. These regional relations suggest that the entire 100 km long pluton is a wedge-shaped body tilted to the east, which has been confirmed by detailed gravity surveys across the body (Richards & Collins, 2004).

Three areas of the Kameruka Suite, located in Fig. 1, were studied in detail: (1) in the Bega River (Fig. 2) where excellent exposures provide a nearly continuous section across the central part of the Kameruka pluton; (2) at Illawambra Weir (Fig. 3) where a swarm

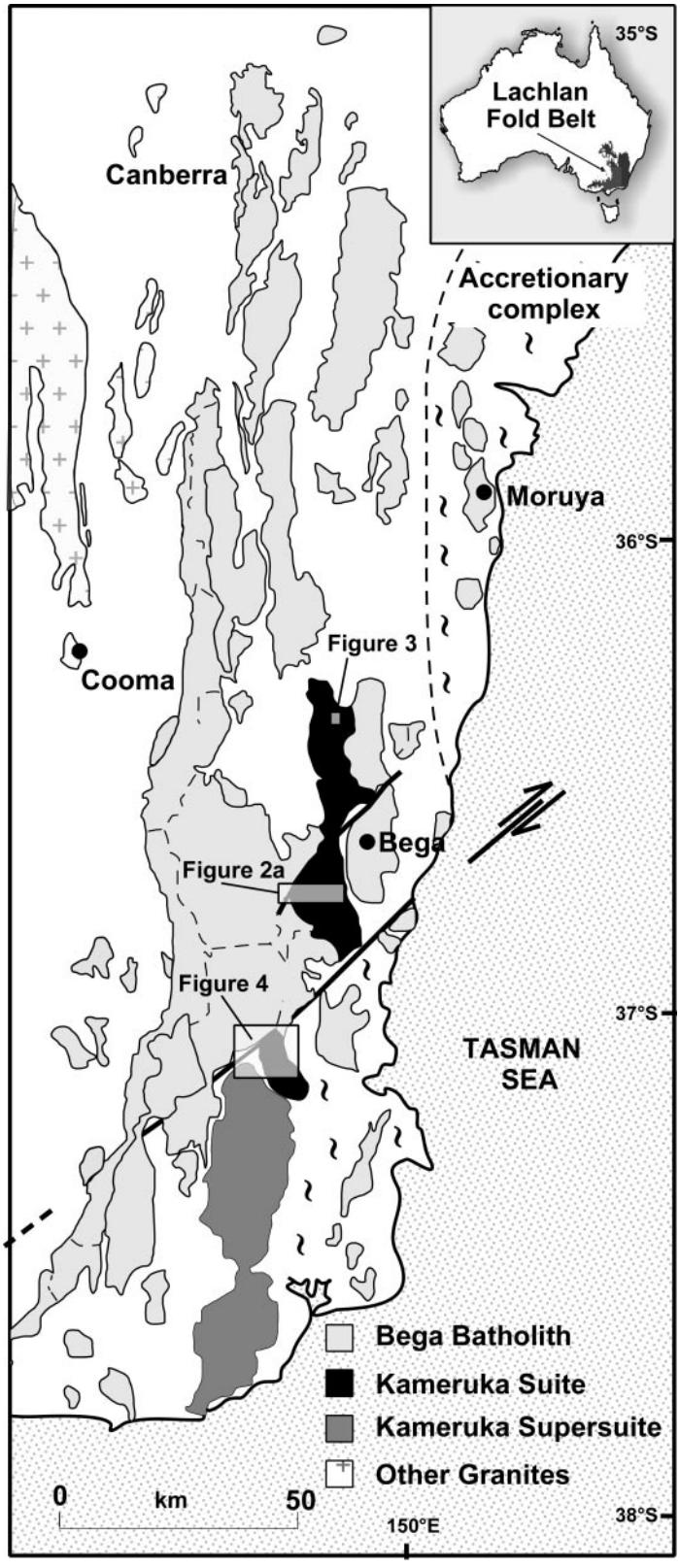

Fig. 1. Simplified geological map of the Bega Batholith highlighting the Kameruka Suite plutons within the Kameruka Super-suite. Rectangles indicate the locations of the detailed study areas.

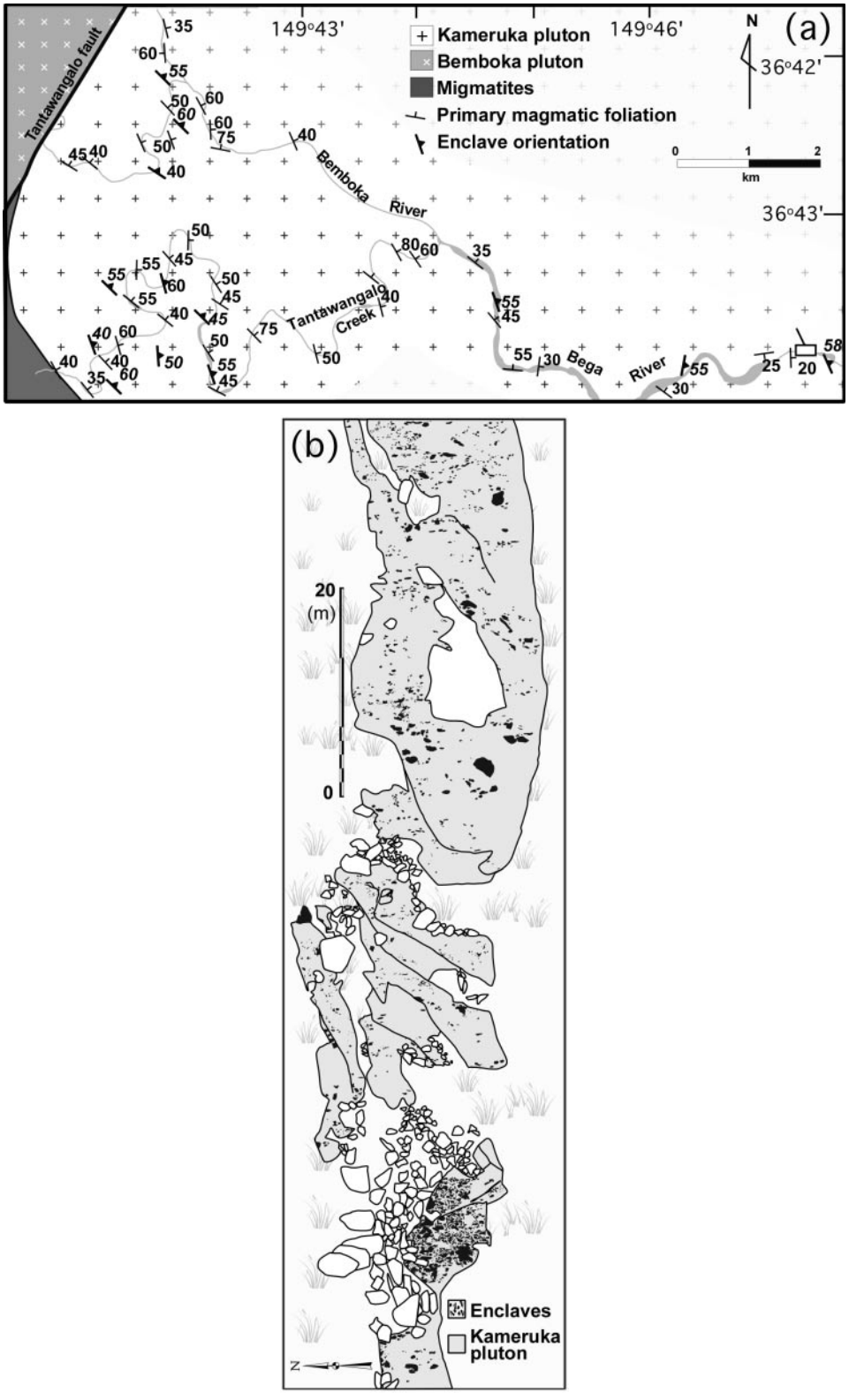

Fig. 2. (a) Geological map of the Bega River channel across the Kameruka pluton. (For location, see Fig. 1.) (b) Detailed sketch map of the Bega River gorge, located at the eastern extremity of (a), showing the consistent north–south orientation of enclaves and a distinctive enclave cluster near the base (west) of the section. Metre-scale polygons are boulders. Grey shaded area is bedrock. (See text for details.)

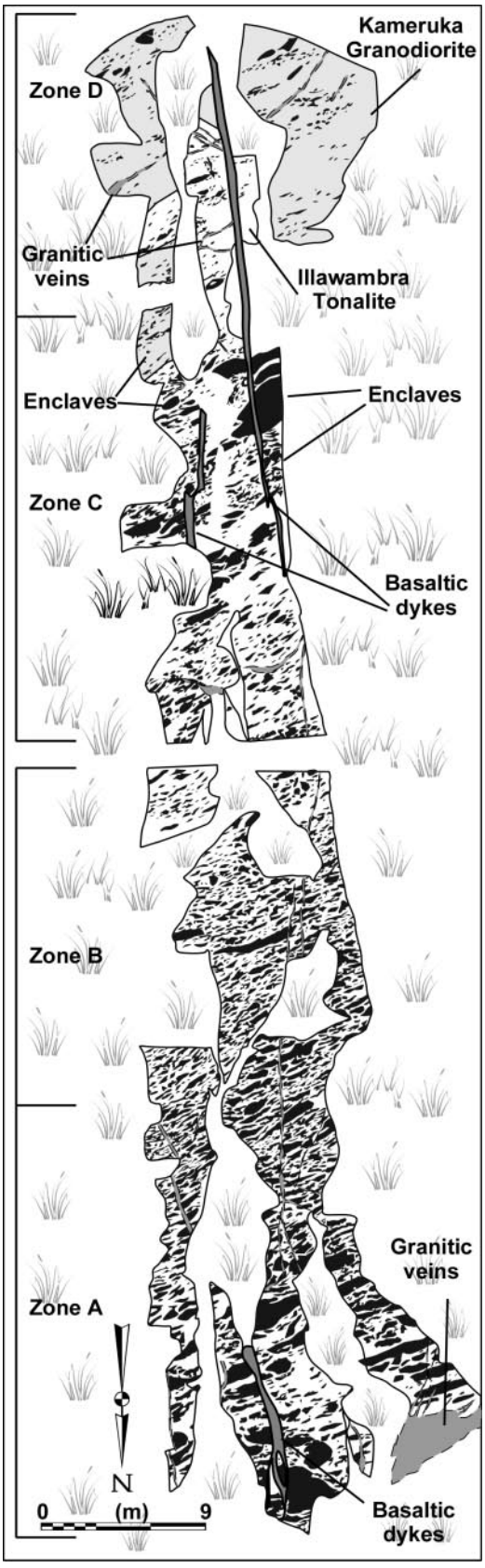

of close-packed, aligned mafic enclaves and tonalitic host are exposed in a spectacular 125 m long section; (3) in the Towamba River drainage basin (Fig. 4) where several river gorge sections provide evidence for pluton construction and replenishment at the base of the pluton.

Bega River section

A near-complete section across the Kameruka intrusion (Fig. 2a) shows that the dominant planar fabric in the granite strikes mainly north–south to NW–SE and dips steeply to moderately (70–40°) to the NE. Coarse feldspars commonly define the planar fabric, which is generally concordant with any planar enclave swarms and biotite-rich schlieren. Gradational boundaries between phenocryst-rich and phenocryst-poor varieties of the granodiorite also commonly parallel the foliation. Just west of the contact within the migmatites (Fig. 2a), narrow sheets of granite lack alkali feldspar phenocrysts, but to the east, the pluton boundary is marked by an abrupt increase in alkali feldspar phenocryst content (up to 10–20% by volume) within a matrix resembling the granite sheets in the migmatite. The 20 mm long phenocrysts are uniform in size and lack plagioclase rims. Only further eastward, after the occurrence of major zones of mafic enclaves, do a significant proportion of the alkali feldspars have plagioclase rims.

Silicic (74–76 wt % SiO_2) and rare mafic (46–50 wt % SiO_2) dykes occur throughout this section, but are most common near the western contacts. Some of the mafic dykes, typically a few metres thick, have irregular curved margins and are back-veined, suggesting that they are syn-magmatic with crystallization of the granite. Silicic dykes vary between 1 and 30 m thick and also have curved and crenulate margins, which suggests that they too were contemporaneous with crystallization of the granite.

Enclave swarms occur at several locations (e.g. Fig. 2b) and are generally concordant with the primary east-dipping foliation. Measured approximately perpendicular to strike, some zones with >50% enclaves are up to tens of metres thick; individual enclaves in these zones may be as large as several metres and range from strongly chilled homogeneous mafic material to complexly mixed hybrid material (Fig. 5). The same variety of enclaves exists in larger (kilometre long), but less concentrated swarms (<10% enclaves), and it reflects the range of smaller (<10 cm diameter) enclaves that are scattered throughout the pluton.

Fig. 3. Detailed geological map of the Illawambra Weir showing the highly aligned and flattened geometry of the enclaves. (See text for details.)

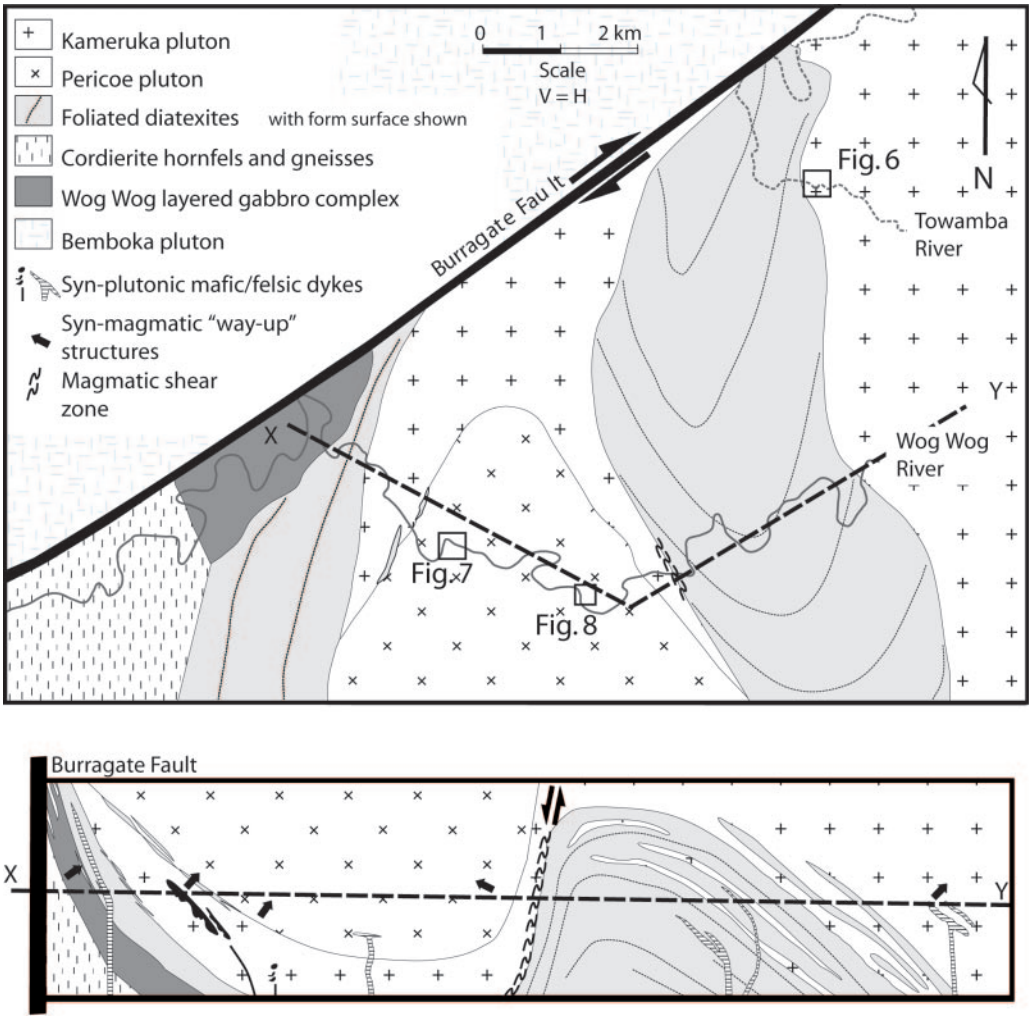

Fig. 4. Towamba River basin: geological map and cross-section. (For location, see Fig. 1.)

Illawambra Weir

The common granitic host of enclaves at Illawambra Weir (Fig. 3) is not typical of the even-grained adamellite that makes up most of the Illawambra pluton (Beams, 1980; Lewis *et al.*, 1994). Rather, it is a dark grey megacrystic tonalite that texturally resembles parts of the Kameruka pluton, but is more mafic, containing a greater proportion of biotite and plagioclase and lesser amounts of megacrystic K-feldspar and quartz. K-feldspar megacrysts appear corroded and partially resorbed, or completely pseudomorphed by sodic plagioclase, so that they are invariably white rather than the typical pink colour of K-feldspar in the Kameruka granodiorite.

Porphyritic Kameruka-type granodiorite is the dominant granite at the southern end of the exposure and is intermingled with a megacryst-poor tonalitic phase, more typical of the enclave host. An irregular, transitional contact between the two granitic phases is defined only by the absence of K-feldspar megacrysts, because the texture of the matrix does not change. Furthermore, aligned mafic enclaves straddle the contact. These features can be interpreted to reflect simultaneous emplacement of the mingled enclaves and host tonalitic phase into the Kameruka magma chamber, where this material commingled with resident crystal mush and then underwent compaction.

Towamba River basin

Some 35 km south of the Bega River, the base of the Kameruka pluton is also exposed in the Towamba River, where the underlying country rock is similarly characterized by migmatites and concordant metre-scale granite sheets (Fig. 4). Over a 50 m interval at the basal contact, granite sheets become more abundant and

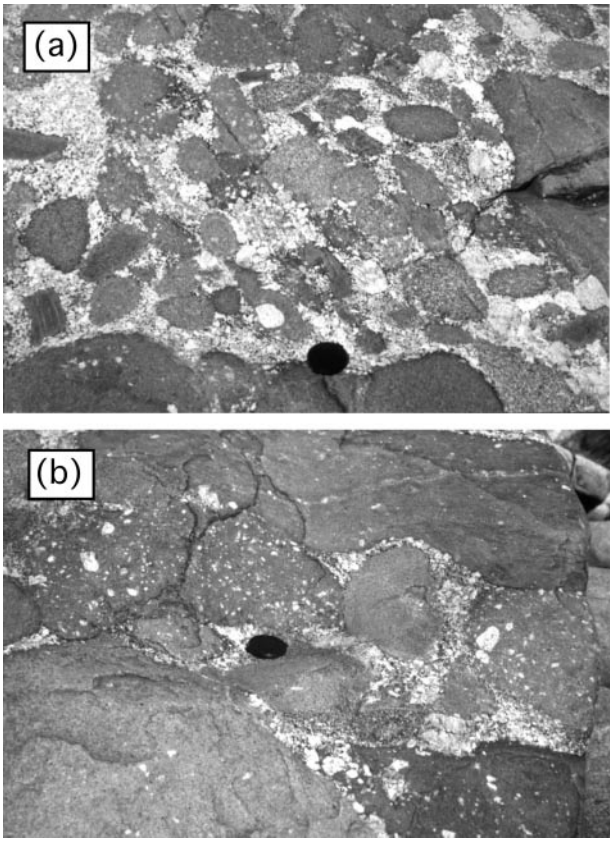

Fig. 5. Field photographs of granite textures in the Kameruka pluton at KSS-2. (a) Variably chilled enclaves, most of which are moulded against large feldspar crystals. (b) Tightly packed enclaves strongly moulded against each other, probably as a result of compaction. Several enclaves have prominent xenocrysts of large K-feldspars derived from the host Kameruka pluton.

discrete semi-concordant rafts of migmatite become less coherent and less laterally continuous.

At this locality, metre-scale felsic, mafic and composite dykes display both cross-cutting, intrusive and mixing relations with the host Kameruka granite, indicating dyke injection contemporaneous with pluton crystallization (Collins *et al.*, 2000*a*). One microgranite dyke can be traced for several hundred metres from the pluton base to a point where it spreads laterally (Fig. 6). The dyke migrated around a rigid metasedimentary raft, aligned subconcordantly with the granite layering (and pluton contact), and propagated another 50 m before terminating as a lens-shaped felsic layer, also oriented subconcordantly with the basal pluton. The lower contact of the felsic layer is distinctive and slightly lobate downward, defined by a sharp compositional and textural change, whereas the top is gradational over several metres to the overlying coarser-grained host-rock that resembles the Kameruka granite. All trace of the original dyke is lost along strike, but it is overlain by a series of stacked, irregular, east-dipping microgranitoid layers, separated by biotite-rich schlieren (Fig. 6). The layers have a similar texture to the dyke and are laterally continuous for >50 m. We suggest that this is a zone of silicic replenishment, fed by the felsic dyke, into the melt-rich part of the magma chamber and along its soft, mushy base.

The basal contact of the Kameruka pluton is also well exposed at three locations along the Wog Wog River. The easternmost contact dips gently to the east, and is the southern continuation of that observed in the Towamba River some 4 km farther north (Fig. 4). Further west, the east-dipping migmatites and granite sheets outline a kilometre-scale half-graben high, with a steep western limb resembling an antithetic growth fault (Richards & Collins, 2004).The basal pluton contact reappears several kilometres upstream, dipping to the west (Fig. 4), and beyond that, the Pericoe and Kameruka granite phases outcrop semi-continuously until the third, westernmost, east-dipping basal contact is reached ~4 km upstream. Based on a larger-scale gravity survey, these relations suggest that the Kameruka pluton comprises two wedge-shaped bodies, thickening to the east (Richards & Collins, 2004), with the Pericoe phase occupying the upper part of the western wedge.

Upward from the westernmost basal contact (Fig. 4), a 300 m thick sheet of megacrystic granite (Kameruka phase) grades to an even-grained homogeneous phase (Pericoe) as K-feldspar megacrysts systematically decrease in size and abundance (Barrett, 1998). Above this, a complex, 600 m thick zone separates the Kameruka sheet from the main Pericoe body. The zone contains a diverse, chaotic array of lenses, dykes and rafts of various sizes and rock type, some hosted by basaltic rock. One large (120 m × 80 m) raft within this 'chaos zone' consists of hornblende-rich tonalite, which resembles the Candelo pluton of Beams (1980). The raft has a semi-continuous rind of porphyritic Kameruka granodiorite, which has also infilled fractures in the raft (Fig. 7). The contact between the Kameruka rind and host Pericoe-type granite (adamellite) is gradational, suggesting that they were coeval magmas. Swarms of mafic enclaves occur both below and above the large raft. A few metres of fine- to coarse-grained, strongly banded, leucocratic granite occurs at the western (lower) contact, separating the raft from the host granite and an underlying enclave swarm. This leucocratic phase also forms apophyses that intrude the raft, the underlying Pericoe-type granite and the mafic enclave swarm. The mafic enclave swarms are moulded around salients and embayments in the block, indicating that they were partially molten when the raft came to rest. These relations are consistent with a depositional system involving sinking and accumulation of differing materials (xenoliths), indicating aggradation to the east.

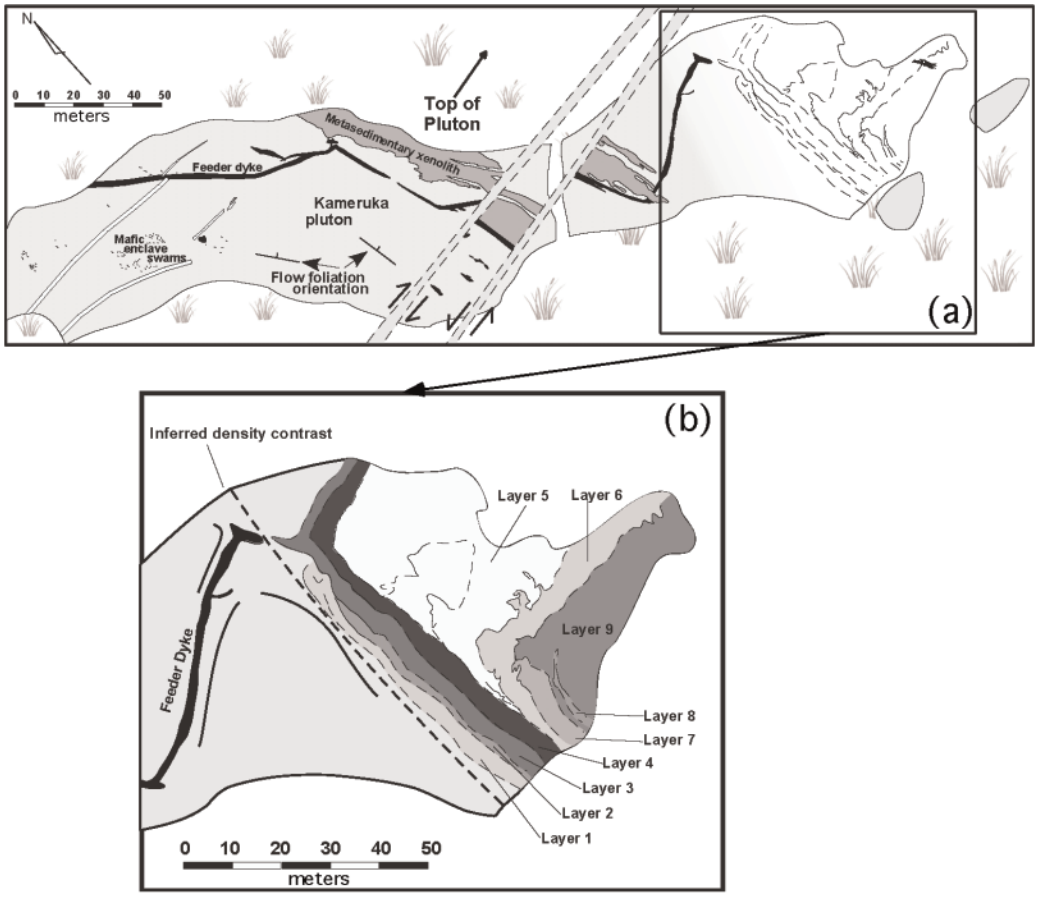

Fig. 6. Sketch map of granitic 'feeder' dykes in the Kameruka pluton showing the changing character from a sharply discordant metre-scale feature (left) into a more diffuse layered sequence to the east (right), concordant with metasedimentary rafts and magmatic foliations in the granite. (a) Location and geometry of compositional and textural boundaries; (b) interpretation of the boundaries shown in (a) as semi-continuous layers aligned sub-parallel to the magma chamber floor. (For location, see Fig. 4.)

Some 20 m farther up section, a series of regular compositional layers resemble 'sedimentary cross-bedded laminations' (Fig. 7). The centimetre-scale, rhythmic layers are compositionally graded with concentrations of biotite and subordinate plagioclase at the base relative to quartz and alkali-feldspar. As such, they resemble sets of graded beds. Some layers are curvi-planar and form cuspate sets that are truncated by overlying cuspate sets. These truncations between cuspate sets of laminae resemble trough cross-bedded units of clastic sediments and suggest that younging of the sequence is upward, to the east, the same as that determined from most other 'way-up' indicators in the pluton.

Channel-like deposits of tightly packed, small (10–20 cm) rounded, well-sorted, mafic enclaves provide additional way-up indicators in the Pericoe granite (Fig. 8). In the even-grained and otherwise massive, homogeneous pink granite, these spectacular dark features show an irregular, lobate base characterized by larger enclaves (up to 50 cm), with preferential compaction against the underlying granite, and a subtle upward decrease in the density of packing. As with the other swarms, they appear to have been deposited at a rheological boundary on crystal-rich mush below crystal-poor magma. The way-up direction of these channels is consistent with the overall upward-facing nature of the Pericoe body (Fig. 4).

Enclaves and enclave swarms

Two areas of enclave swarms in the northern part of the map area were studied in detail: one in the Bega River section (Fig. 2) though the Kameruka pluton, the other in the Illawambra pluton (Fig. 3). Typically, background proportions of enclaves within the pluton are 1–3%; these are 5–10 cm in diameter, but range up to 10 m in some swarms.

A detailed map of a 140 m long section of the Bega River (Fig. 2b) shows that two types of enclave swarms exist (Ellison, 1999): a series of low-density (up to 50%

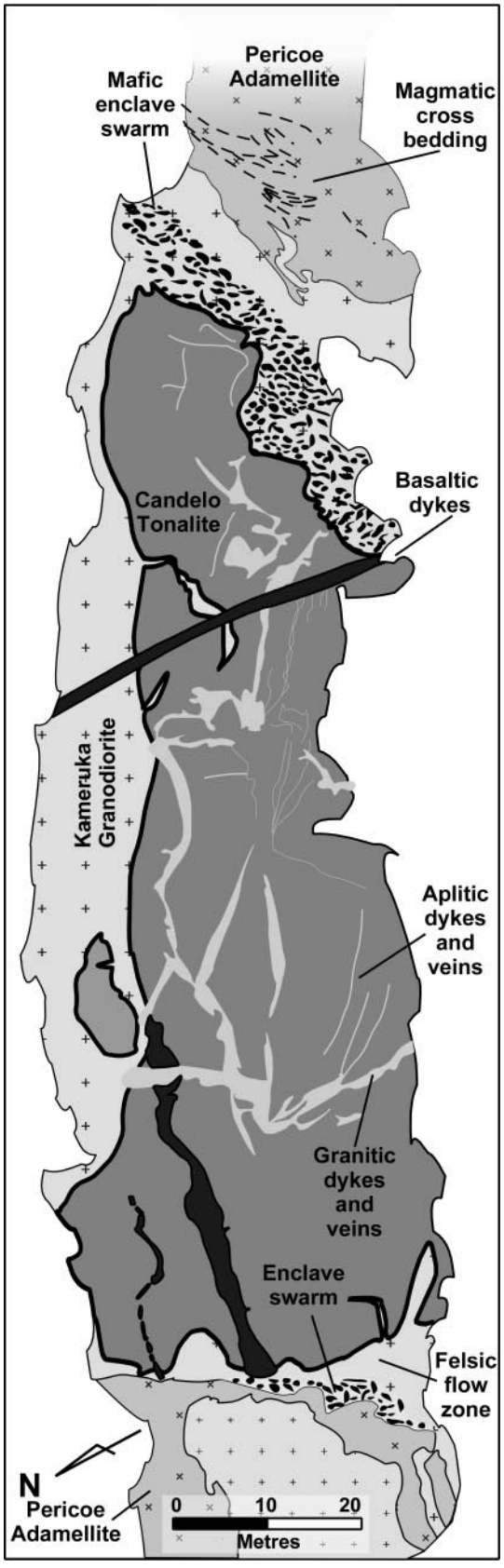

enclaves), subparallel swarms that strike north–south and dip 30–50° to the east, and an apparently more equant, high-density (up to 70–80% enclaves) swarm at the western edge of the map (Fig. 2b). The low-density types consist of diffuse enclave 'trails' that can be traced 50–70 m semi-continuously across the outcrop, parallel to layering defined by feldspars. Individual enclaves are elongate subparallel to the trail and have aspect ratios of 2:1 to 5:1. They are moderately well-sorted, ranging from 5 cm to ~2 m in length. Larger enclaves, up to 10 m long, exist as isolated, subrounded to elongate blobs between the layers. Some of the enclaves have convex to lobate bases, and occur on a bed of K-feldspar and plagioclase megacrysts; others are moulded against one another. The enclaves in the high-density swarm are arranged into layers dipping about 30° to the SE, slightly oblique to the north–south-striking swarms.

The enclave swarm studied in the Illawambra pluton (Fig. 3) consists of enclaves that are more abundant, larger (10 cm to >10 m length), and more densely packed than in the Bega River swarm (Ellison, 1999). Enclaves have variable size and shape, and many contain alkali feldspar xenocrysts. They are usually elongate, the majority with aspect ratios >3:1 and aligned concordantly to a strongly developed NE-trending magmatic foliation defined by plagioclase, which dips 45–55° to the SE. Many enclaves are moulded against one another, tending to be flatter on the SE contact and more irregular to lobate on the NW side.

Concentrations of tightly packed feldspar aggregates on the NW side of individual enclaves within the swarm appear to reflect compaction and removal of interstitial melt during settling of the enclaves. As such, they appear to be way-up indicators (Wiebe, 1996; Wiebe & Collins, 1998) showing younging to the SE. This is consistent with the occurrence of small (centimetre)-scale 'flame structures' of tonalite that pierce the NW edges of some of the mafic enclaves (Ellison, 1999), suggesting buoyant rise of felsic material through the mafic layers. The flatter (upper) SE and lobate (lower) NW contacts give an asymmetry consistent with enclave sinking in the granite host, as described elsewhere (Wiebe & Collins, 1998). Also, the lower (northern) half of the swarm appears to show an upward decrease in size and abundance of enclaves (Fig. 3), possibly reflecting 'fining upward' similar to that observed within density currents formed in sedimentary environments. All these features imply that way-up is to the SE, in the general direction ascertained for the entire Kameruka pluton.

Fig. 7. Detailed map of the Candelo tonalite mega-xenolith in the Kameruka pluton. (See text for description and significance; for location, see Fig. 4.)

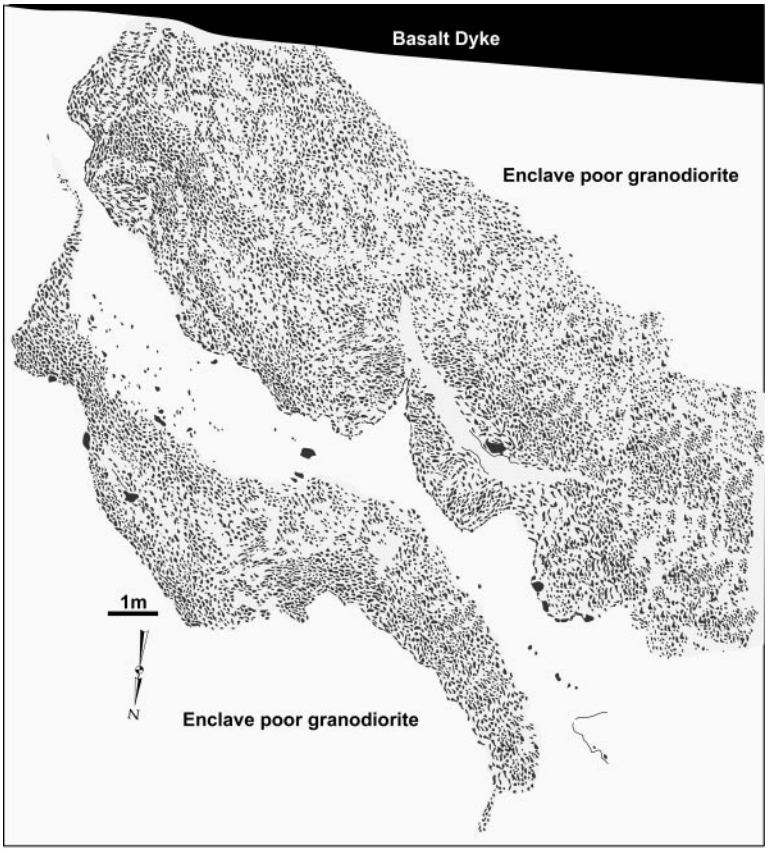

Fig. 8. Detailed map of channel-shaped enclave swarms in the Pericoe pluton. Channel geometry is highlighted by a concave base with flattened and densely packed enclaves grading upwards (SW) where enclaves are scattered throughout the granite. Additionally, scour-type structures are evident on the NE margin and thin trails of enclaves propagate laterally from the channel margins. Overlying enclave swarms (channels) locally depress and deform earlier deposited enclaves. These structures suggest way-up to the SE, consistent with a location on the eastern limb of a synform (see Fig. 6).

Interpretation

Enclave swarms typically have features that indicate that they were deposited at a rheological boundary, resting on granitic crystal mush (Wiebe & Collins, 1998). Several aspects of these swarms provide way-up indicators including: (1) compaction of the underlying crystal mush; (2) impression of chilled mafic material down into the interstices between larger crystals; (3) infiltration of granitic interstitial melt into the overlying mafic bodies; (4) upward from the base, a gradational decrease in the abundance and size of the enclaves. These way-up features have been found at many locations across the pluton, and all of these features indicate top to the east (right-way-up). The distribution of these structures suggests that this entire section of the Kameruka pluton was deposited sequentially from the western margin eastward. The contrasting nature of these contacts, from concordant and migmatitic in the west, to sharply discordant hornfelsed country rock in the east, suggests a western basal contact and a sidewall contact in the east, consistent with growth of the pluton from base (west) to top (eastward).

Enclave compositions vary from gabbro to diorite, quartz diorite and tonalite, reflecting progressive increases in quartz and feldspar xenocryst content. The presence of ovoid to embayed K-feldspar and quartz grains within enclaves (Fig. 5b) of basaltic or granitic composition, indicates that they formed by mixing between mafic magma and resident crystal-bearing granitic magma (see Hibbard, 1991). Mixing probably occurred elsewhere in the chamber, prior to mingling with the host granite (Collins *et al.*, 2000*a*). The prominence of plagioclase rims on some K-feldspar megacrysts also indicates that magma mixing was responsible for the development of sporadic rapakivi-textured granite in the Kameruka pluton.

PETROGRAPHY

The Kameruka granodiorite is a medium- to coarse-grained unit dominated by quartz, plagioclase, alkali

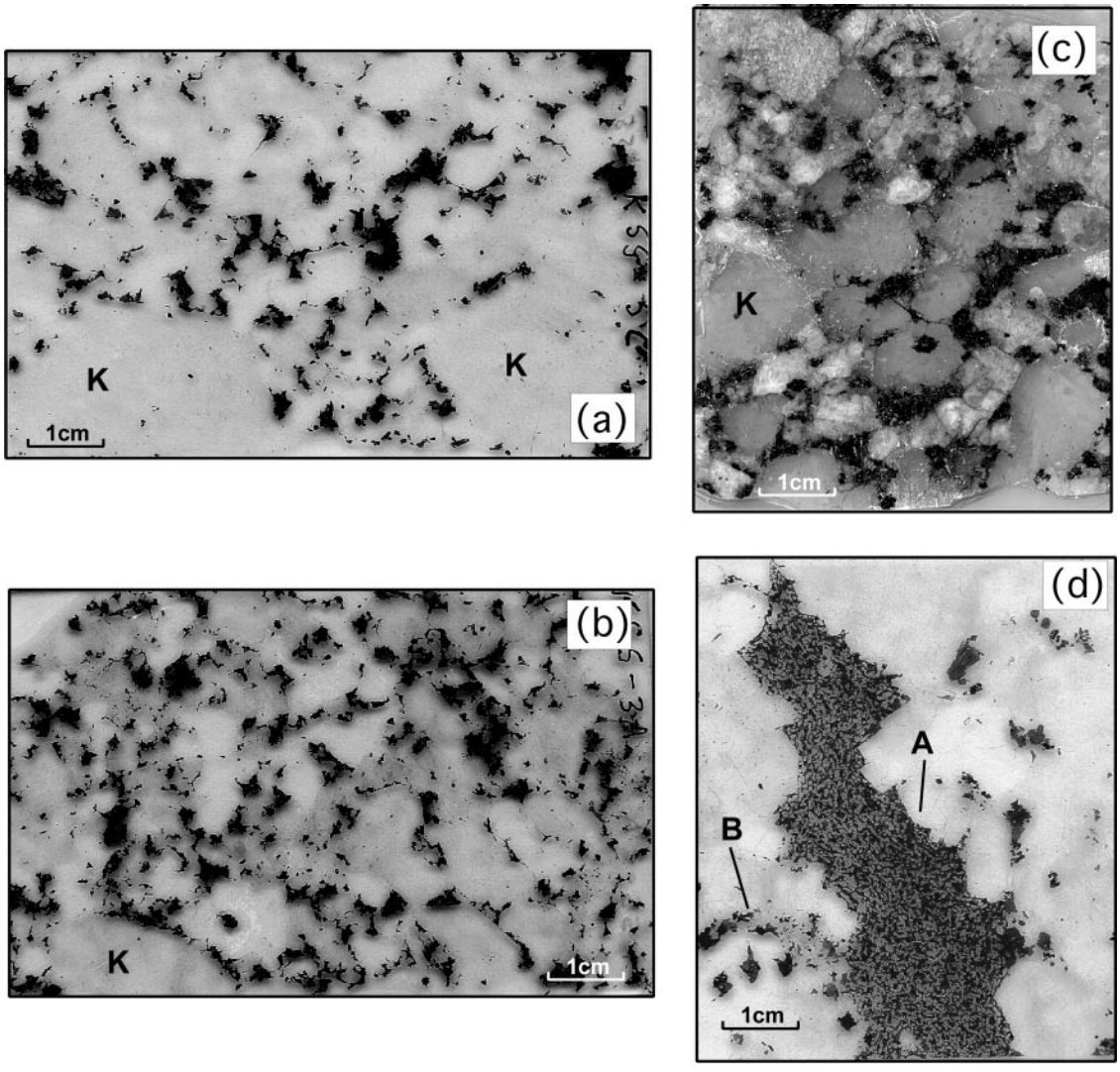

Fig. 9. (a–c) Thin-section photographs of Kameruka granodiorite showing cumulate textures. Black is biotite, white is plagioclase, K is megacrystic K-feldspar, and the remainder includes quartz and fine-grained felsic minerals. (Note the location of biotite within interstices between cumulate felsic minerals, including megacrysts.) (d) Interstitial relation of small hornblende-rich mafic enclave to felsic minerals, indicating injection and solidification in a granitic cumulate. (See text for explanation of A and B.) Location is the Bega River section in Fig. 2a.

feldspar and biotite. Alkali feldspar occurs widely, both as prominent phenocrysts that vary in length from about 20 to 100 mm, and as interstitial grains. The texture is also characterized by equant quartz crystals, commonly 5–15 mm in diameter, and tabular white plagioclase mostly between 5 and 20 mm in length (Fig. 9a). Biotite typically occurs as clusters of small grains (<3 mm) that are partly deformed and appear to fill the interstices between the larger feldspar and quartz, irrespective of colour index (Fig. 9a–c). Modal variation locally extends to granitic and tonalitic compositions. Colour index ranges mostly between 10 and 20, and accessory phases, closely associated with biotite, include apatite, opaque minerals, allanite and zircon in decreasing abundances. Hornblende is absent, as it is in the Pericoe phase and the granite dykes. Except for the general absence of alkali feldspar megacrysts, the Illawambra pluton closely resembles the Kameruka pluton.

Alkali feldspar varies widely in size, abundance and complexity, even within a single outcrop or hand-specimen; it may be locally concentrated in some areas and sparse in others. Whereas some phenocrysts are euhedral, with or without overgrowths into the interstices of adjacent grains, other crystals commonly have plagioclase rims of varying thickness. Where alkali feldspar occurs within, or closely associated with, mafic enclaves, plagioclase rims are present on most of the crystals. Some phenocrysts are completely

pseudomorphed by plagioclase (albite) and quartz. Uncommon, ovoid to subhedral plagioclase grains (both in the enclaves and disseminated within granite far from enclaves) consist of many small, aligned, zoned plagioclase crystals intergrown with quartz and biotite; some of these grains have small, irregular and corroded cores of alkali feldspar. In the western Bega River section, the inferred lower part of the Kameruka pluton, rapakivi grains are scarce to absent and K-feldspar is subrectangular (K in Fig. 9c), whereas in the more eastern parts of the section, all varieties of the alkali feldspar megacrysts commonly occur in the same outcrop, and they are usually round or ovoid (K in Fig. 9a and b).

Plagioclase is complexly zoned with many delicate oscillations and with normally zoned rims of variable thickness. The compositional range lies mostly between An_{40} and An_{25}. Thin reversed zones commonly truncate inner zones and develop a euhedral form outward; these appear to represent episodes of corrosion followed by crystallization of more calcic plagioclase. As noted in many granitic rocks, the sequences of compositional zoning vary widely for different grains within the same thin section (Wiebe, 1968).

The Pericoe pluton is a medium-grained, biotite granite that generally lacks alkali feldspar phenocrysts. Plagioclase shows a similar compositional range ($An_{40–20}$) and similar style of zoning to Kameruka. Accessory phases include apatite, opaque minerals, zircon and prominent monazite surrounded by strong pleochroic haloes in biotite. Sericite alteration is common and some larger grains of interstitial to poikilitic muscovite occur in some samples.

The fine-grained granitic dykes are homogeneous and contain subhedral plagioclase, alkali feldspar and equant quartz with grain sizes between 0·3 and 1 mm. The texture contrasts with the granites in that many of the grains are anhedral, and intergrown as a polygonal mosaic. Plagioclase shows simple normal zoning with scarce faint oscillations, no corrosional reverse zones and only scarce sodic patches that connect to the normally zoned rims. Small subhedral biotite inclusions occur rarely in plagioclase. Accessory minerals include apatite, opaque minerals, zircon and possibly monazite. Sericite alteration and some small interstitial muscovite grains occur in most dykes.

The syn-magmatic mafic dykes are very fine-grained and dominated by thin tabular plagioclase and sub-ophitic to interstitial hornblende. Biotite is variable, but low in abundance. Very fine-grained Fe–Ti oxides and apatite are uniformly disseminated.

Mafic to intermediate enclaves reflect interaction between felsic and mafic magma. The enclaves have fine-grained textures and most commonly are dominated by subhedral stubby plagioclase and biotite, with lesser hornblende. The texture resembles that of the syn-magmatic mafic dykes. Larger enclaves tend to be dominated by hornblende rather than biotite.

ANALYTICAL METHODS

Fresh rock (5–10 kg) was crushed to a fine powder using a tungsten-tipped hydraulic splitter and mill. The powder was fused into a chemically homogeneous glass disc using lithium metaborate flux, and a duplicate disc was similarly prepared. Both samples were analysed by polarized energy-dispersive X-ray fluorescence (ED-XRF) using a Spectro X'Lab 2000 system at the University of Newcastle, Australia. For isotope analysis, 100 mg sample aliquots were spiked with mixed $^{85}Rb/^{84}Sr$ and $^{147}Sm/^{150}Nd$ enriched spike solution and dissolved in steel-jacketed Teflon vessels using HF, HNO_3 and HCl. A two-step digestion process was used involving heating the sample to dryness then adding fresh acids and placement in an oven at 200°C overnight. overnight. Ion exchange pre-concentration procedures follow Potts (1987). Cation-resin ion exchange columns were utilized and solutions were loaded onto Ta–Re filaments before evaporation. A Finnigan Mat 261 mass spectrometer was used for isotopic compositions and element concentrations, and standards were calibrated following Bennett *et al.* (1993).

Mineral analyses were carried out by laser ablation–inductively coupled plasma mass spectrometry (LA–ICP-MS) using a Merchantek LUV266 LA system coupled with a Hewlett Packard 4500 quadrupole ICP-MS system at the GEMOC National Key Centre, Macquarie University, Australia. Thick section (~50 μm) ablation points were registered using an optical microscope coupled with a computer-driven sample stage to provide co-registered *x–y* co-ordinates. The samples were then carbon coated before placement in the sample chamber. The beam was focused through a petrographic microscope onto the sample with typical spot size from 20 to 50 μm and analysis was run for 200 s. A 1:1 ratio of argon to helium was used to transfer the analyte to the ICP-MS system prior to flushing with argon for 60 s. NIST 610 and 612 glasses were retained as external standards. Mineral compositions determined by ICP-MS have trace element analyses to sub-ppm levels, with a reported precision of less than 5%. Online data-reduction was done using Glitter software (Jackson, 2001).

GEOCHEMISTRY

Representative major and trace element compositions of plagioclase, alkali-feldspar, biotite and apatite from a sample of the Kameruka granodiorite were obtained by

Table 1: Electron microprobe and LA–ICP-MS data for cumulus minerals in KSS-5C, a typical granodiorite from the Kameruka pluton

	plag	kspar	biotite	apatite
SiO_2	61·31	64·12	34·97	0·06
Al_2O_3	24·07	18·43	15·24	0·00
TiO_2			4·07	0·02
FeO	0·11	0·06	23·76	0·18
MnO			0·31	0·26
MgO			8·01	0·00
CaO	5·82	0·04	0·00	55·26
Na_2O	7·37	0·55	0·10	0·14
K_2O	1·61	16·02	9·47	0·01
P_2O_5			0·02	41·90
Cl			0·09	0·07
F			0·34	2·74
Total	100·30	99·22	96·37	100·64
ppm				
Ba	146	5920	1457	4
Rb	3	306	766	1
Sr	508	419	1	176
Pb	21·3	54·0	3	6
Nb			82	0
Y			0	2860
La	16·1	1·8	0	327
Ce	23·3	1·5	1	1150
Eu	2·2	2·1		
Nd			0	992
Sc			67	0
V			417	1
Co			44	0
Ni			46	0
Ga	28	108	67	1

electron microprobe and LA–ICP-MS at Macquarie University (Table 1). In addition, 21 new chemical analyses of the Kameruka granodiorite, the Pericoe adamellite and related fine-grained granitic dykes were obtained by XRF analysis at the University of Newcastle (Table 2). These analyses, together with data from Beams (1980), are plotted on selected Harker variation diagrams in Fig. 10.

Granitic rocks of the Kameruka Suite, including the contemporaneous fine-grained granitic dykes (Table 2), range from about 67 to 76 wt % SiO_2, with the Kameruka pluton having the lowest silica (67–73% SiO_2) and the dykes having the highest (75–76% SiO_2). For most major and some trace elements (e.g. Sr) plotted against silica the four groups of rocks define a single, approximately linear trend. Some trace elements increase (e.g. Pb) or decrease (e.g. Ce) markedly at the high-SiO_2 end (Fig. 10). Other elements show considerable scatter from the linear trend (e.g. Ba, Y). Careful evaluation of the diagrams suggests that there are real differences in the chemical trends between the Kameruka, Illawambra and Pericoe plutons. The Pericoe shows the greatest divergence, with variations to much higher concentrations of Ba, La, Ce, Th and Zr (Fig. 10). Granitic dykes have the lowest concentrations of FeO, MgO, CaO, Ba, Sr, Ce and Y, and the highest concentrations of K_2O and Rb (Fig. 10). The relative scarcity of samples between 72 and 73% SiO_2 may reflect sampling bias. The relatively large scatter of alkalis appears to be consistent with the highly variable proportions of feldspars and the variable development of plagioclase rims on K-feldspar. The large scatter of many trace elements may reflect erratic distribution of accessory phases. The granitic dykes show significant systematic variation in some major and several trace elements: as silica increases, CaO, Na_2O, FeO, Sr, Th and V all decrease, whereas K_2O, Rb and Pb increase (Fig. 10).

The granitic dykes plot in a tight group near the 1 kbar minimum in the system quartz–albite–orthoclase–H_2O (Fig. 11). The Pericoe and Illawambra samples plot close to the dykes, slightly shifted toward the Q–Ab join (Fig. 11). The Kameruka granitoids mostly plot further toward the Q–Ab join and are scattered well into both the quartz and feldspar fields. In the Bega River section near the western (lower) margin, the Kameruka pluton has 72·9% SiO_2 and 4·05% K_2O. SiO_2 and K_2O decrease in samples a few kilometres to the east to 71·7% SiO_2 and 2·51% K_2O. However, a sample from near the eastern (upper) margin, located directly above the enclave swarms described in Fig. 2, has 69·3% SiO_2 and 2·79% K_2O. These variations suggest that there is no simple compositional zoning throughout the intrusion, but that compositions might relate to proximity of mafic replenishments.

Representative syn-plutonic mafic dykes and mafic to intermediate magmatic enclaves were also analysed to characterize the contemporaneous, more mafic, material associated with the Kameruka pluton (Table 3). The chilled gabbroic rocks and mafic dykes (46–52 wt % SiO_2) have basaltic compositions that lie off the linear trend of the Kameruka Suite at the low SiO_2 end for most elements (Fig. 12). MgO ranges from 7 to 10 wt % and large variations in TiO_2 and P_2O_5 also occur. Most enclaves have between 57 and 67 wt % SiO_2 and are much more scattered than the granites on Harker plots (Fig. 12). The enclave array connects with the low-SiO_2 end of the granite array, and overlaps the mafic dykes cluster in wt % SiO_2 for most elements, although MgO is higher and Al_2O_3 and Na_2O are lower. Some mafic

Table 2: Major and trace element compositions of granites from the Kameruka, Pericoe and Illawambra plutons and granitic dykes

	KSS-2A KAM	KSS-5C KAM	KSS-7A KAM	KSS-8B KAM	DB2 KAM	DB4 KAM	DB6 KAM	DB8 KAM	DB11 KAM	DB12 KAM	DB13 KAM	BH26 PERICOE	BH27 PERICOE	AB139 PERICOE
SiO_2	67·88	70·08	71·37	71·48	69·73	68·96	69·10	67·09	68·19	67·60	67·80	71·72	71·90	72·44
TiO_2	0·64	0·56	0·42	0·37	0·59	0·64	0·60	0·68	0·69	0·72	0·77	0·48	0·41	0·48
Al_2O_3	14·40	13·53	13·73	13·72	14·23	14·45	14·47	14·89	14·54	14·57	14·80	13·82	13·71	12·73
Fe_2O_3	4·39	3·89	2·92	2·74	3·97	4·35	4·18	4·78	4·38	4·66	4·67	2·87	2·66	2·93
FeO	0·00	0·00	0·00	0·00	0·00	0·00	0·00	0·00	0·00	0·00	0·00	0·00	0·00	0·00
MnO	0·07	0·06	0·06	0·06	0·06	0·06	0·06	0·07	0·06	0·06	0·06	0·02	0·02	0·04
MgO	1·47	1·28	1·02	0·86	1·33	1·38	1·32	1·72	1·60	1·70	1·72	0·88	0·74	0·80
CaO	2·98	2·58	2·37	1·50	2·94	3·07	2·95	3·70	3·28	3·34	3·83	2·24	2·04	1·84
Na_2O	3·18	3·16	3·42	3·24	3·34	3·24	3·25	3·56	3·34	3·29	3·41	3·09	3·12	2·93
K_2O	2·73	2·45	2·96	3·97	2·25	2·71	3·02	2·05	2·24	2·37	1·97	3·52	3·99	4·03
P_2O_5	0·19	0·16	0·14	0·12	0·12	0·19	0·18	0·19	0·19	0·20	0·20	0·13	0·11	0·12
LOI	0·86	1·19	1·09	1·02	0·84	0·59	0·63	0·80	1·05	1·09	0·59	0·67	0·84	n.d.
Total	98·79	98·94	99·50	99·08	99·40	99·64	99·76	99·53	99·56	99·60	99·82	99·44	99·54	98·34
Ba	748	588	608	773	576	690	793	407	563	602	570	2196	1725	1180
Rb	115	107	119	162	112	123	125	115	118	122	102	101	97	112
Sr	289	239	236	208	228	274	272	272	298	282	308	228	200	196
Pb	15	17	16	22	17	20	19	12	15	14	12	22	23	16
Th	12·5	18·5	10·4	18·3	20	13	15	8	13	11	9	30	31·5	15·8
U	2·1	1·1	3·1	3	n.d.	n.d.	n.d.	n.d.	n.d.	n.d.	n.d.	2	5	1·2
Zr	237	216	176	168	220	228	216	218	235	252	254	267	241	247
Nb	11·8	11·4	10·2	11·2	3	9·5	7·3	3	6·5	7	4	2	5	8
Y	23	28	20	26	42	17	18	17	16	16	15	20	20	16
La	38·6	41·5	19	37·4	39	26	33	18	35	19·5	41·5	92·5	67·5	45
Ce	75·3	81	37·7	74·8	53	32	45·7	27	46	50·5	61·5	95·5	84·5	92
Sc	13	11	7	9	n.d.	n.d.	n.d.	n.d.	n.d.	n.d.	n.d.	n.d.	n.d.	n.d.
V	69	63	41	40	44	67	71	74	76	79	73	24	26	35
Cr	14	20	9	12	8	14	13	67	21	6	16	2	5	5
Co	77	51	79	55	n.d.	n.d.	n.d.	n.d.	n.d.	n.d.	n.d.	104	100	7
Ni	0	0	0	0	4	4	6	6	6	4	5	1	3	2
Cu	0	0	0	0	2	7	9	2	8	2	6	1	3	6
Zn	57	48	40	39	59	65	61	69	62	64	64	13	17	42
Ga	17	16	16	16	15	17	15	15	16	16	15	41	36	14

	AB207 PERICOE	DB1 PERICOE	DB9 PERICOE	DB18 PERICOE	AB335 ILLAWA	AB336 ILLAWA	AB337 ILLAWA	AB338 ILLAWA	AB339 ILLAWA	BH24 granitic dyke	BH1 granitic dyke	BH7 granitic dyke	BH12 granitic dyke	BH25 granitic dyke
SiO_2	73·74	72·20	74·18	72·29	72·71	74·88	73·57	71·21	73·20	75·45	75·28	74·96	74·6	75·45
TiO_2	0·29	0·35	0·28	0·38	0·36	0·25	0·29	0·42	0·35	0·19	0·17	0·19	0·19	0·21
Al_2O_3	12·79	13·62	12·57	13·32	13·65	13·06	13·24	14·06	13·37	13·11	13·39	13·32	13·51	13·29
Fe_2O_3	1·92	2·42	1·91	2·53	0·81	0·85	0·77	0·86	0·78	1·14	1·37	1·58	1·61	1·29
FeO	0·00	0·00	0·00	0·00	1·50	0·95	1·26	1·80	1·56	0·00	0·00	0·00	0·00	0·00
MnO	0·04	0·04	0·02	0·03	0·05	0·03	0·04	0·05	0·04	0·01	0·03	0·03	0·03	0·01
MgO	0·52	0·78	0·55	0·67	0·63	0·40	0·48	0·75	0·56	0·42	0·49	0·44	0·41	0·41
CaO	1·34	1·41	1·34	1·56	2·02	1·26	1·54	2·23	1·72	0·9	0·7	1·27	1·35	1·19
Na_2O	3·24	2·69	2·56	3·13	3·49	3·21	3·24	3·53	3·25	2·53	2·99	3·02	3·21	2·83
K_2O	4·41	4·75	4·69	4·20	3·61	4·52	4·25	3·56	4·04	5·13	4·37	4·27	3·99	4·45
P_2O_5	0·06	0·15	0·10	0·10	0·11	0·07	0·08	0·14	0·09	0·09	0·06	0·06	0·05	0·08
LOI	n.d.	n.d.	n.d.	n.d.	n.d.	n.d.	n.d.	n.d.	n.d.	0·73	0·95	0·6	0·7	0·86
Total	98·35	98·41	98·20	98·21	98·94	99·48	98·76	98·61	98·96	99·71	99·77	99·72	99·65	100·05
Ba	580	729	1250	2286	810	785	805	805	950	620	385·5	609·5	619·5	627
Rb	165	230	122	141	138	150	144	183	136	189	184·5	203	193·5	163·5
Sr	104	101	180	168	213	150	171	226	194	82	87·5	140	170·5	115·5
Pb	16	28	28	28	22	25	23	19	21	38	42·5	31·5	33·5	37
Th	22·8	24·3	25	45·3	16	22	22	15	25	10	21	24	28·5	22·5
U	3	3	3	3	1	2	2	2	2	5	2	2	2	2
Zr	161	183	184	234	180	158	174	198	213	98	78	102·5	108	119
Nb	10·5	5	3·7	3	10	10	9	13	9	2	2	2	6	5
Y	25	22	16	27	29	32	25	23	33	16	21	19·5	21	23·5
La	38	44·3	52·3	81·3	27	32	35	27	41	22	22·5	27	16·5	24·5
Ce	80	70	60·3	99	62	75	80	58	92	36	35·5	59	49·5	46·5
Sc	n.d.	n.d.	n.d.	n.d.	n.d.	n.d.	n.d.	n.d.	n.d.	n.d.	n.d.	n.d.	n.d.	n.d.
V	16	22	12	27	27	27	16	21	34	1	9·5	22	14	14
Cr	3	3	3	3	5	4	5	7	6	2	2	2	2	2
Co	3	66	69	68	5	3	5	6	5	100	115	73·5	108	102·5
Ni	2	2	3	2	2	1	2	4	2	1	1	1	1	1
Cu	0	2	2	2	2	1	2	2	2	1	1	1	1	1
Zn	26	41	26	37	37	30	35	44	40	20	16	26	21	18·5
Ga	14	13	12	12	17	15	15	18	15	14	22	23	28	23

KAM, Kameruka granodiorite; PERICOE, Pericoe adamellite; ILLAWA, Illawambra granodiorite; LOI, loss on ignition; n.d., not determined.

dykes in the Bega River section have compositions comparable with those of the enclaves. This suggests a general affinity of the Bega and Illawambra enclaves with the syn-magmatic mafic dykes; however, the consistently lower MgO (Fig. 12), Ni and Cr at similar SiO_2 content suggests that the enclave mafic magma was generally more fractionated (Fig. 12).

Nd and Sr whole-rock isotopic compositions were determined for representative samples of the Pericoe and Kameruka plutons and for mafic and granitic dykes (Table 4). A plot of εNd vs $^{87}Sr/^{86}Sr_i$ (Fig. 13) indicates that the mafic dykes have compositions consistent with other mantle-derived mafic rocks from the Bega Batholith, with εNd +3 to +4 and $^{87}Sr/^{86}Sr_i$ between 0·703 and 0·705, whereas the granitic dykes have much lower εNd (–5 to –6) and higher $^{87}Sr/^{86}Sr_i$ (0·704–0·711). The initial $^{87}Sr/^{86}Sr$ isotopic composition of the granites and basalts varies between 0·7045 and 0·7055, although the felsic dykes (and one Pericoe sample) range to 0·710. The Pericoe and Kameruka plutons also show a similar cluster in isotopic composition between εNd of –3 to –4. The most silica-rich samples from both plutons overlap with the lower εNd values (–5 to –6) of the felsic dyke rocks. Thus, a general trend of decreasing εNd with

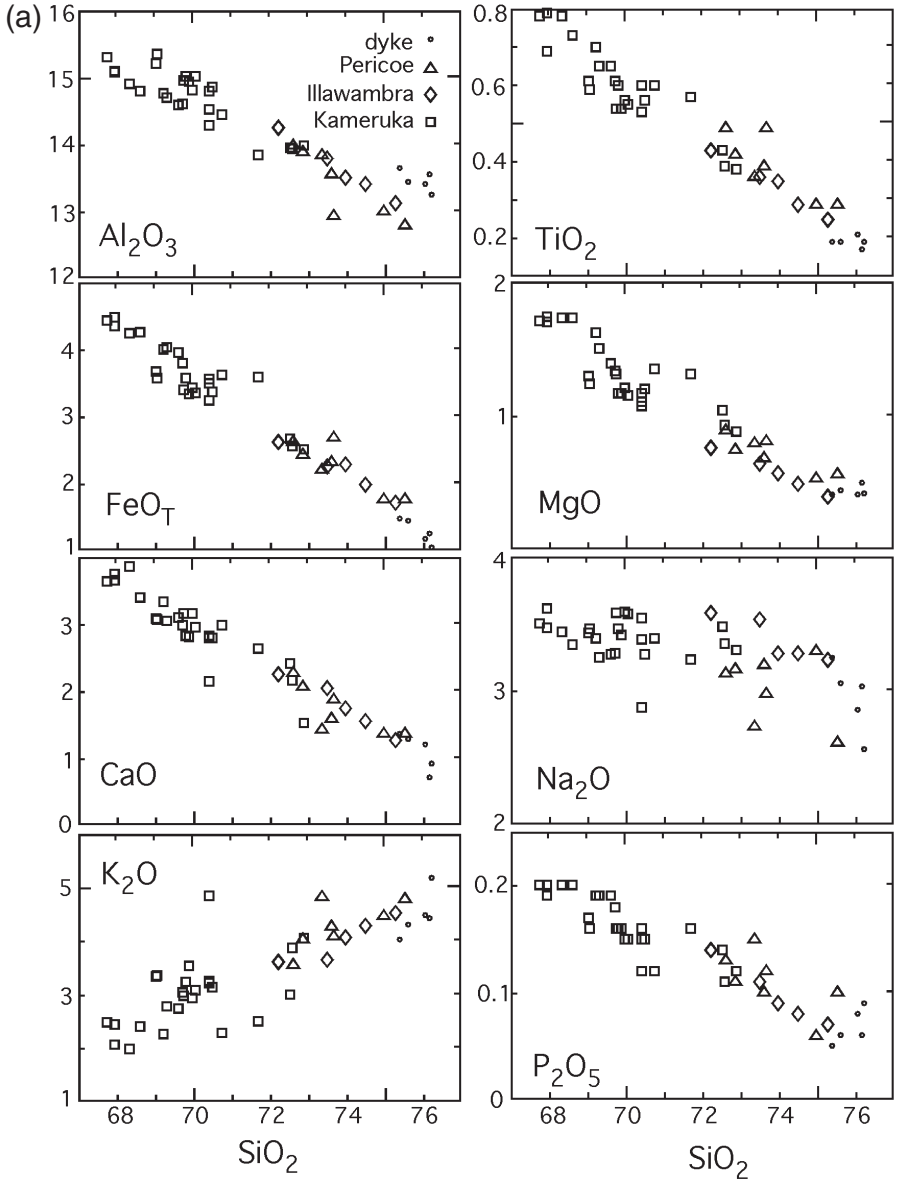

Fig. 10. Harker variation diagrams for the Kameruka, Illawambra and Pericoe granites and granitic dykes. (a) Major elements; (b) selected trace elements.

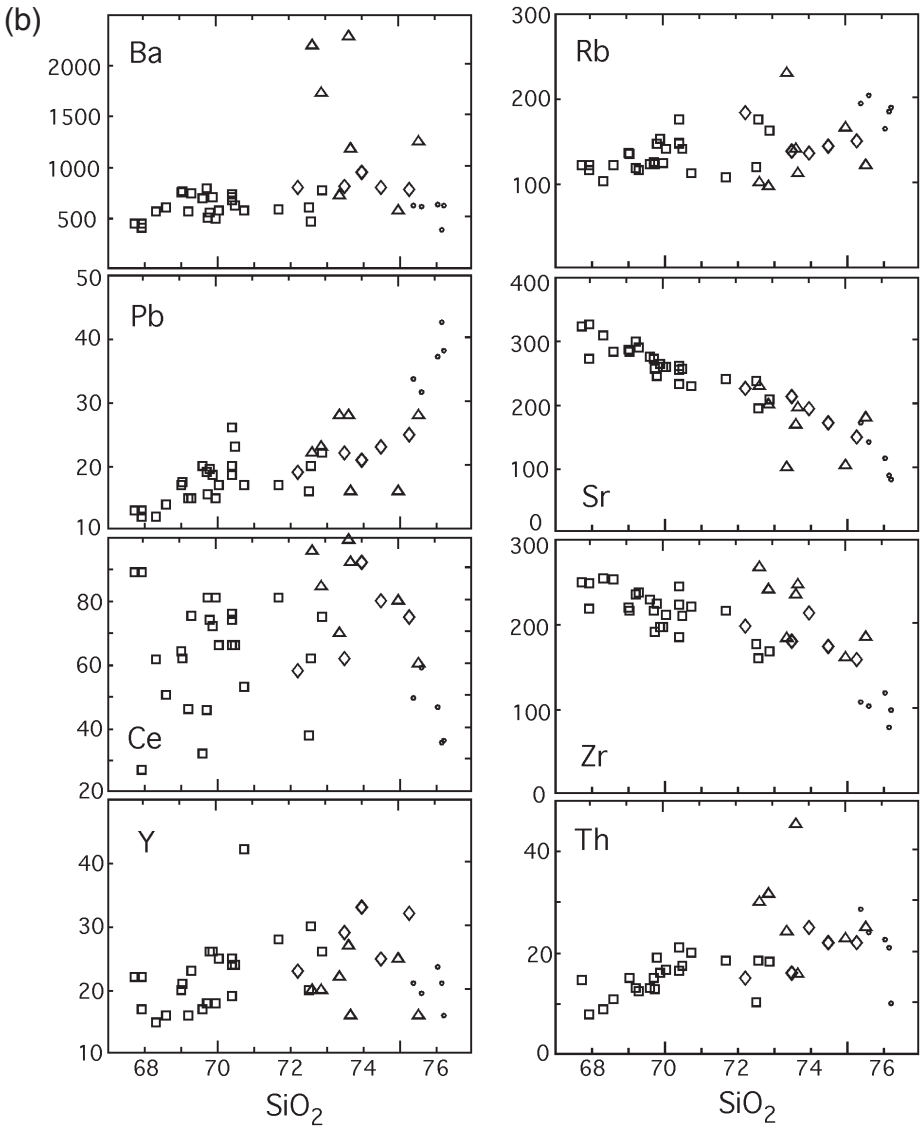

Fig. 10. *Continued.*

increasing silica content exists, but each compositional group clusters around a similar isotopic value, precluding a simple mixing model whereby chemical variation is solely caused by differing proportions of mafic–silicic inputs.

The higher $^{87}Sr/^{86}Sr_i$ and lower εNd of the felsic dykes relative to the Kameruka Suite granites could result from preferential contamination of the dykes as they pass through the migmatites. Locally, granitic dykes have migrated along leucosome-rich stroma, which increases the likelihood of mixing between the two silicic magmas. This possibility cannot be resolved with the present dataset, although the near-constant εNd values of the dykes, which are markedly different from those of the metasediments (Fig. 14), argues against contamination. Irrespective, the initial isotopic ratios of the Kameruka and Pericoe granitic rocks form a cluster that lies between the compositions of the mafic and felsic dykes, consistent with field and petrographic relations suggesting that the plutons were dyke-fed, with a maximum local contribution of 30% from the mafic component.

EVIDENCE FOR CRYSTAL ACCUMULATION ON A MAGMA CHAMBER FLOOR

We consider that the textures dominant in the Kameruka pluton (comparable with those illustrated in

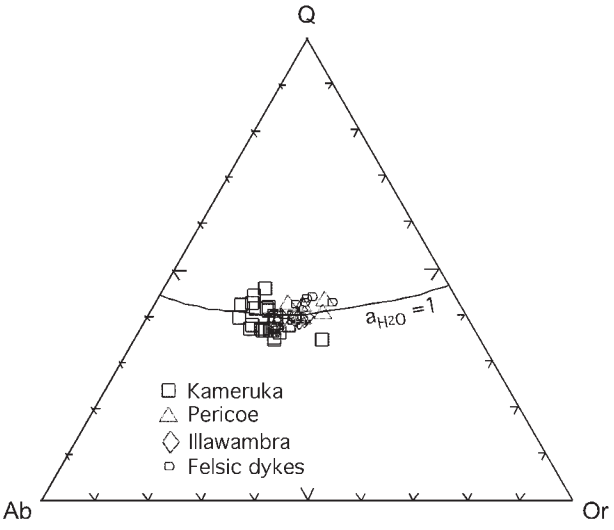

Fig. 11. The system quartz–albite–orthoclase–H_2O showing the projected compositions of the Kameruka, Pericoe and Illawambra granites and granitic dykes. Bold line is H_2O-saturated cotectic at 1 kbar.

Fig. 9) can best be explained by a cumulate model. We interpret the overall texture as that of a touching framework of subhedral cumulus minerals with overgrowths and smaller crystals of the same minerals filling the interstices (Fig. 9). These textures can be described in parallel terms to those used for mafic cumulate rocks in mafic–ultramafic layered intrusions (Irvine, 1982). The cumulus minerals in a typical granite from the lower part of the Kameruka intrusion, and within the Pericoe and Illawambra intrusions, consist of large, mostly subhedral grains of plagioclase, alkali feldspar, quartz, biotite and apatite. Variable amounts of trapped intercumulus liquid produced overgrowths on the cumulus minerals (e.g. visible as normally zoned rims on plagioclase) and finer-grained material that apparently nucleated interstitially from the melt.

The textural argument for accumulation of crystals and loss of liquid in samples of the Kameruka granite is supported by the typically contrasted sequences of internal zoning in adjacent alkali feldspar (and, more subtly, plagioclase) crystals. This can be observed at microscopic, hand-specimen and outcrop scale, as described above. The contrasted zoning and reaction shown by these crystals reflect very different crystallization histories (changes of thermal or chemical environment through time). Although different zoning patterns can develop in adjacent plagioclase grains during *in situ* growth, the effect is generally subtle and does not explain the major resorption zones in some alkali feldspar megacrysts, let alone why adjacent megacrysts show no such effects. It requires that the rocks represent concentrations of crystals that formed from different liquids, which presumably developed in different locations within the magma chamber before the grains were brought together. In other words, the rocks must be cumulates.

Field relations provide the main evidence that the Kameruka pluton formed by accumulation of crystals on the floor of a silicic magma chamber. Of central importance are the widespread occurrences of outcrop-scale features that suggest deposition, particularly layers of enclave swarms resting on dense accumulations of large feldspar crystals, such as at Illawambra Weir (Fig. 3), and, on a smaller scale, enclaves moulded around feldspar grains (Fig. 9d). The fine grain size of the mafic material indicates rapid cooling and suggests that it entered the cooler magma chamber very shortly before coming to rest on the granite. Where chilled mafic enclaves have commingled with granitic magma, the fine-grained mafic material is commonly impressed into this framework of cumulus minerals (A in Fig. 9d) at the bottom of the inclusion. However, at the top of this inclusion, the mafic material has been expelled into an interstice, displacing and locally mixed with the coeval felsic interstitial melt (B in Fig. 9d). Figure 9d also shows that the cumulus minerals are commonly pressed more tightly together when enclaves settle upon them, probably because the denser mafic material has compacted the granitic crystal–liquid mush during settling, thereby removing most of the interstitial liquid (Wiebe & Collins, 1998). The close proximity of mineral grains on the bottom side in the granite host (A in Fig. 9d) suggests that the granitic material on which the mafic material rests was already a touching framework of quartz–feldspar crystals.

The large rafts of migmatite and exotic granite blocks at the base of the Pericoe pluton, which were probably stoped from the walls or roof of the magma chamber, also support the existence of a crystal-rich chamber floor. In particular, the large raft of Candelo tonalite (Fig. 7) can be interpreted as a large stoped block that fractured itself and the underlying mush when it impacted on the chamber floor. Evidence for fracturing at this stage is the presence of Kameruka-type granitic dykes in the block, which grade into aplite eastward (upward), but which do not extend beyond the block on that upper side. In contrast, the aplite–pegmatite phase at the base of the block intruded both the block and the underlying host-Pericoe phase, indicating that the base became sufficiently viscous to fracture transiently. This strongly flow-banded and texturally variable aplitic phase may represent interstitial melt that was filter-pressed from the underlying crystal mush, eventually fracturing that mush as the local fluid pressure increased rapidly during impact of the raft with the chamber floor.

In contrast, features in the granite immediately above the Candelo tonalite raft support the existence of crystal-poor magma overlying the floor. The unusual sequence

Table 3: Compositions of mafic and intermediate enclaves in the Kameruka suite and related syn-magmatic mafic dykes

	Mafic dykes and chilled gabbro										Enclaves in the Illawambra adamellite										
Sample:	DB5	DB7	DB10A	MKB70	MKB71	MKB73	MKB75	5A	5B	3A	PE24	PE25	PE26	PE28	PE30	PE31	PE32	PE34	PE35	PE36	PE37
SiO_2	49·23	48·39	48·99	49·98	49·55	49·33	49·51	44·40	46·56	48·05	57·17	57·28	63·68	50·22	67·05	57·32	67·68	63·60	65·03	60·32	61·38
TiO_2	1·36	1·50	1·37	1·39	1·26	0·66	0·53	2·69	2·00	2·46	0·92	1·22	0·57	1·14	0·64	1·01	0·60	0·78	0·70	0·88	0·87
Al_2O_3	15·48	15·69	16·61	16·23	16·2	16·21	17·11	15·73	16·04	13·95	17·73	16·82	17·09	18·92	15·45	16·67	15·45	15·73	15·66	17·61	16·27
Fe_2O_3	10·09	10·13	10·38	10·09	9·9	8·54	8·15	13·69	12·02	12·71	7·37	8·10	4·68	10·80	4·37	7·58	4·13	5·58	5·08	7·23	6·25
MnO	0·16	0·16	0·17	0·16	0·15	0·14	0·14	0·21	0·19	0·16	0·13	0·13	0·08	0·16	0·05	0·13	0·05	0·09	0·08	0·07	0·10
MgO	9·29	8·87	8·40	7·36	7·45	9·21	9·11	6·69	7·50	6·73	3·32	2·94	1·93	3·82	1·73	3·44	1·33	2·59	2·11	1·59	2·84
CaO	9·46	8·97	10·78	9·41	9·56	12·07	12·49	8·96	10·00	8·74	7·30	6·81	5·31	8·11	4·77	7·20	3·70	5·11	4·55	5·03	6·00
Na_2O	2·37	2·52	0·68	2·42	2·29	1·71	1·65	2·36	1·98	3·11	3·20	3·37	3·63	2·76	2·97	3·25	3·86	3·05	3·35	3·93	3·16
K_2O	0·64	1·73	0·68	0·71	0·65	0·18	0·16	0·46	0·35	0·83	1·46	1·19	1·64	1·91	1·58	1·38	1·87	1·88	1·90	1·73	1·72
P_2O_5	0·24	0·27	0·24	0·15	0·17	0·05	1·03	0·55	0·30	0·42	0·21	0·47	0·17	0·27	0·18	0·34	0·19	0·21	0·20	0·28	0·24
LOI	1·03	1·30	0·97	1·84	2·41	1·43	0·03	3·99	3·24	2·62	0·77	1·15	0·62	2·04	0·88	0·98	0·62	0·95	0·81	0·88	0·67
Total	99·35	99·53	99·27	99·74	99·59	99·53	99·91	99·73	100·18	99·78	99·58	99·48	99·40	100·15	99·67	99·30	99·48	99·57	99·47	99·55	99·50
Ba	105	121	167	163	139	39	62	254	154	191	340	400	419	325	399	376	516	448	434	488	415
Rb	24	78	48	37	33	8	6	13	10	49	60	52	84	74	76	60	78	96	96	80	82
Sr	299	304	340	289	248	367	369	280	250	274	474	582	545	467	396	530	380	408	402	503	434
Pb	6	9	8	8	9	6	5	10	7	5	14	14	14	14	9	12	15	12	12	13	14
Th	7	6	5	5	5	6	4	3	1	1	n.d.	n.d.	n.d.	n.d.	n.d.	n.d.	n.d.	n.d.	n.d.	n.d.	n.d.
U	3	3	3	0	0	0	0	0	1	1	n.d.	n.d.	n.d.	n.d.	n.d.	n.d.	n.d.	n.d.	n.d.	n.d.	n.d.
Zr	146	155	119	117	122	23	11	300	188	235	154	228	130	136	160	160	232	158	179	456	167
Nb	8	6	6	3	3	3	3	17	11	13	10	14	5	10	5	6	7	8	7	7	6
Y	28	29	26	27	29	11	9	43	35	40	44	44	18	33	14	33	15	24	19	16	31
La	15	19	13	11	12	9	3	23	11	18	16	22	9	5	16	30	20	16	17	39	30
Ce	42	36	24	24	25	28	15	62	33	41	26	32	28	28	49	43	37	36	39	66	34
Sc	n.d.	n.d.	n.d.	n.d.	n.d.	n.d.	n.d.	29	27	31	n.d.	n.d.	n.d.	n.d.	n.d.	n.d.	n.d.	n.d.	n.d.	n.d.	n.d.
V	202	198	218	210	210	228	209	291	234	304	144	184	82	194	70	175	58	110	87	83	134
Cr	386	312	220	165	147	324	339	238	85	124	6	9	5	5	8	17	7	11	8	5	16
Co	54	51	50	44	47	46	53	38	40	38	n.d.	n.d.	n.d.	n.d.	n.d.	n.d.	n.d.	n.d.	n.d.	n.d.	n.d.
Ni	165	186	102	82	88	85	79	66	66	57	12	9	3	5	3	14	3	12	8	3	12
Cu	43	47	29	35	45	25	38	41	40	38	14	16	3	25	3	30	36	29	16	20	30
Zn	82	85	105	83	81	60	58	125	102	113	73	84	52	98	42	76	40	54	51	62	62
Ga	15	15	16	16	15	12	15	22	21	20	37	36	34	40	34	36	35	34	36	38	36

Table 3: continued

	Enclaves in Kameruka granodiorite from the Bega River area																			
Sample:	PE14	PE15	PE16	PE17	PE18	PE19	PE20	PE21	PE22	PE23	1B	1G	1D	1E	2B	2C	3C	3D	5E	5G
SiO_2	63·14	64·15	61·03	65·42	50·00	59·14	66·19	60·19	63·20	61·64	54·29	53·59	58·50	62·57	65·02	63·08	66·12	59·64	62·73	61·00
TiO_2	1·02	0·96	0·63	0·85	1·08	0·84	0·90	0·79	1·02	0·63	1·19	0·79	0·74	1·22	1·01	1·12	0·75	0·78	0·59	0·85
Al_2O_3	16·22	16·06	16·62	15·69	18·69	17·06	14·90	16·85	16·20	16·46	17·52	16·49	17·04	15·36	15·34	15·86	15·61	16·89	16·24	17·85
Fe_2O_3	6·06	5·72	6·96	5·28	10·82	7·46	5·42	7·10	6·06	6·87	8·88	7·72	6·43	7·34	6·46	6·28	5·20	6·46	4·69	6·69
MnO	0·08	0·09	0·12	0·08	0·17	0·11	0·07	0·11	0·08	0·11	0·16	0·13	0·13	0·12	0·08	0·10	0·10	0·11	0·09	0·07
MgO	1·89	1·83	2·71	1·80	4·22	2·52	1·89	2·38	1·90	2·68	3·59	6·77	3·70	1·98	1·28	1·98	1·32	3·46	3·14	1·50
CaO	4·29	3·98	5·42	3·90	8·44	5·54	3·69	5·29	4·30	5·13	6·92	7·89	6·81	4·74	3·79	4·26	3·52	5·02	5·60	4·13
Na_2O	3·48	3·52	3·03	3·34	2·72	3·01	3·37	3·16	3·47	2·95	3·97	3·38	3·48	3·14	3·79	3·28	3·94	3·00	2·71	4·47
K_2O	2·20	2·34	2·04	2·08	2·12	2·39	2·06	2·21	2·20	2·15	0·77	0·72	1·54	1·88	2·01	2·24	1·87	2·60	1·50	2·01
P_2O_5	0·32	0·32	0·10	0·28	0·22	0·23	0·23	0·22	0·32	0·11	0·38	0·26	0·13	0·30	0·25	0·40	0·24	0·19	0·17	0·26
LOI	0·80	0·80	1·69	1·25	1·19	2·14	0·71	1·32	0·80	1·30	2·11	2·16	1·10	0·89	0·89	1·27	0·93	1·48	2·74	0·74
Total	99·50	99·77	100·35	99·97	99·67	100·44	99·43	99·62	99·55	100·03	99·78	99·90	99·60	99·54	99·92	99·87	99·60	99·63	100·20	99·57
Ba	421	512	293	414	286	475	472	466	434	307	372	284	224	297	641	405	455	341	537	326
Rb	126	131	120	123	102	118	129	118	125	130	15	16	73	114	88	128	141	182	78	108
Sr	342	376	357	344	400	382	308	370	346	322	610	554	376	249	342	338	348	342	394	332
Pb	15	18	15	18	12	12	15	14	17	8·5	8	9	11	9	13	10	9	6	19	18
Th	n.d.	n.d.	n.d.	n.d.	n.d.	n.d.	n.d.	n.d.	n.d.	n.d.	3	3	4	14	11	12	13	9	9	13
U	n.d.	n.d.	n.d.	n.d.	n.d.	n.d.	n.d.	n.d.	n.d.	n.d.	1	1	1	2	1	2	1	2	2	2
Zr	219	238	88	206	103	182	255	176	224	82	113	96	86	182	499	226	296	135	199	459
Nb	10	10	6	10	8	8	8	12	10	5	8	6	6	12	12	15	16	10	11	14
Y	27	32	22	28	32	32	22	30	27	14	20	16	16	33	32	39	36	22	25	31
La	27	29	9	45	7	16	36	16	33	10	13	15	15	34	57	42	33	22	28	39
Ce	53	60	25	54	34	29	50	30	55	30	43	45	32	79	120	98	75	52	70	87
Sc	n.d.	n.d.	n.d.	n.d.	n.d.	n.d.	n.d.	n.d.	n.d.	n.d.	23	23	23	24	15	20	15	17	14	12
V	97	99	148	90	208	113	92	105	93	144	194	178	178	188	86	112	53	115	87	42
Cr	5	5	6	5	5	6	6	5	5	5	8	312	25	3	6	1	34	43	60	9
Co	n.d.	n.d.	n.d.	n.d.	n.d.	n.d.	n.d.	n.d.	n.d.	n.d.	34	39	34	38	43	41	38	42	40	30
Ni	3	4	3	3	6	6	4	4	4	3	13	102	12	0	2	0	0	25	34	2
Cu	16	29	20	26	22	16	6	12	15	14	35	40	42	21	11	40	30	29	17	11
Zn	68	64	68	59	94	75	58	76	68	60	111	74	70	84	76	81	76	78	54	85
Ga	35	36	36	34	42	37	38	36	36	36	20	16	18	19	22	19	20	18	16	25

n.d., not determined.

of graded and trough-like cross-beds at the eastern (top) side of the block (Fig. 7) are similar to compositionally graded layers and cross-beds in sedimentary environments, features that probably formed by traction currents. Similar processes have been proposed for repeated olivine–pyroxene layering in some ultramafic rocks (Irvine, 1974). In both analogous situations, a relatively low-viscosity fluid is essential to permit effective sorting (Gilbert, 1906), so it is likely that a melt-rich zone (magma chamber) existed at the top of the raft during crystallization of these unusual 'bedded' units. The cause of the currents essential for sorting is also probably related to movement of the raft, either as it sank through the chamber or as it settled onto the chamber floor. In any event, the close association between two extremely rare events, settling of a huge (~150 m high) raft and generation of graded and trough cross-beds in granite, seems to imply a cause-and-effect scenario related to sinking and settling of the raft at a major crystal mush–liquid interface in the pluton.

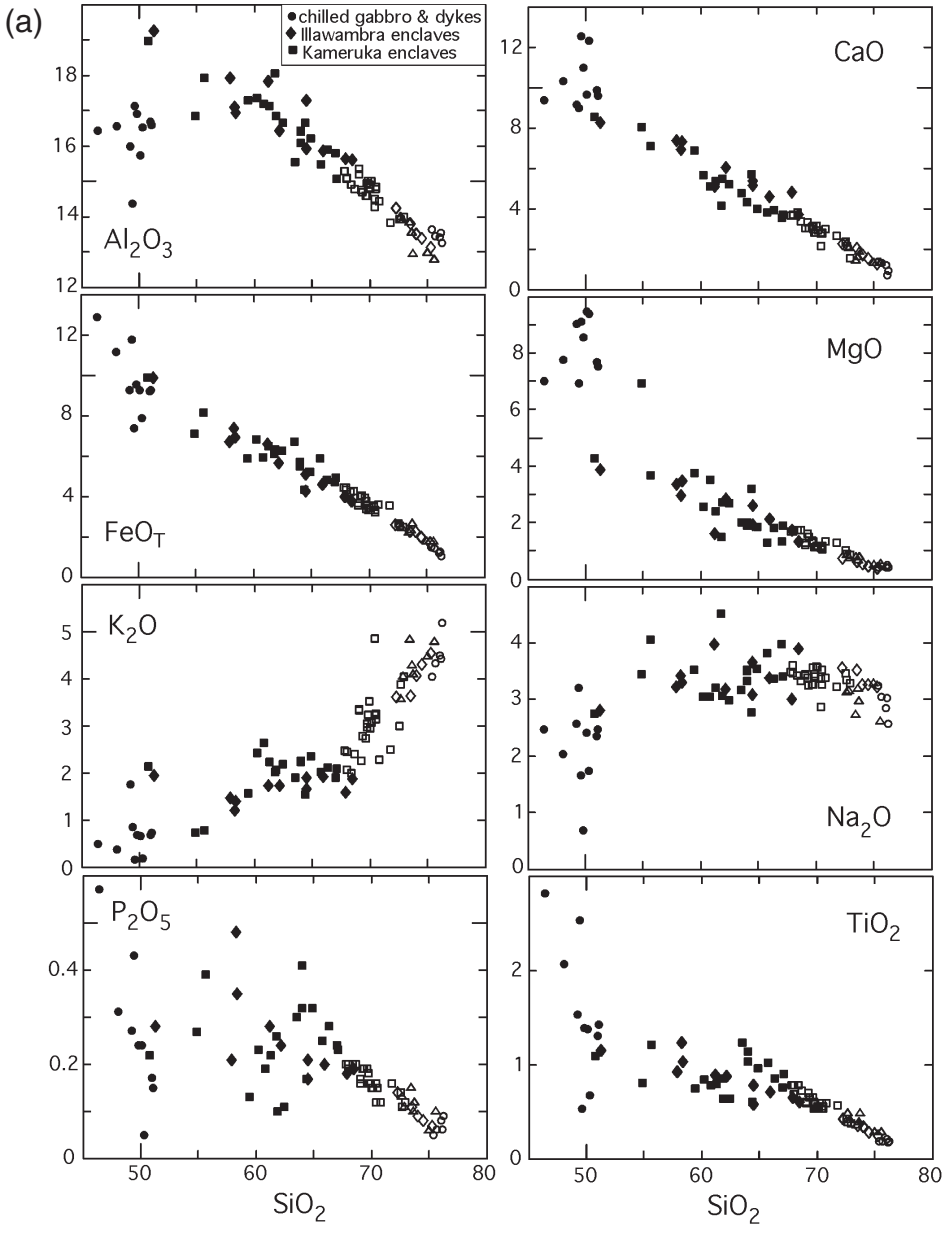

Fig. 12. Harker variation diagrams showing mafic components (filled symbols) compared with Kameruka Suite granites and granitic dykes (open symbols). Mafic components include syn-magmatic basaltic dykes and enclaves. (a) Major elements; (b) trace elements. (See text for discussion.) Open symbols are as in Fig.11.

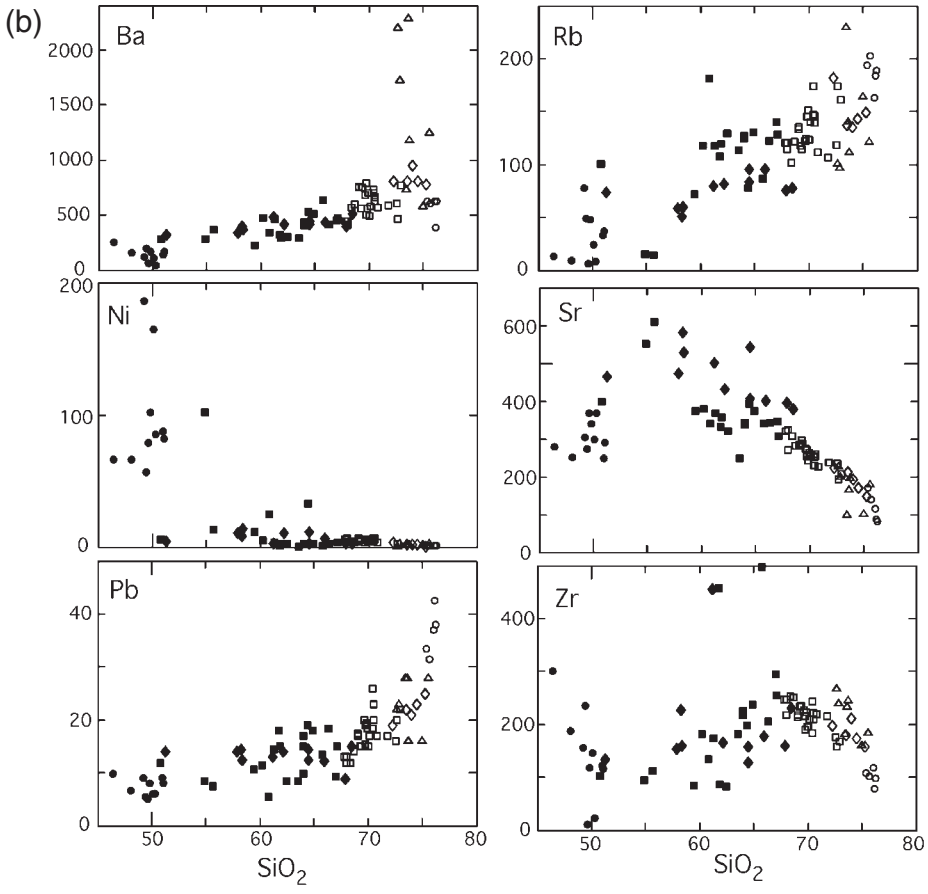

Fig. 12. *Continued.*

Based on the widespread occurrences of east-dipping primary planar features, semi-concordant with mafic enclave swarms and rafts of country rock, the Kameruka pluton appears to have solidified gradually by deposition of crystals on an aggrading floor of a magma chamber. The evidence for compaction of granitic material at the base of these bodies suggests that the floor of the chamber was a rheological boundary or transitional zone between high-viscosity crystal mushes and an overlying crystal-poor magma. It is likely that the thickness of the transition between effectively solid floor and liquid interior varied greatly depending on the history of crystallization and replenishment within the chamber. In other intrusions, load-cast structures at the base of some chilled mafic layers may have diameters of 10 m or more, indicating deformable crystal mush to at least that depth below a crystal-poor magma (Wiebe, 1993).

Although we suggest that the granites are cumulates, we do not infer that the mushes at the floor need to have been produced by settling of individual crystals. Rather, we think it more likely that slurries of crystal mushes may have settled. The expected greater loss of heat along the roof and walls of a chamber (compared with its floor) makes it most likely that nucleation and growth of crystals would be concentrated along these zones, with crystals forming a solidification front (a transitional zone that grades from a solid exterior to a liquid interior; e.g. Marsh, 1988). These packages of crystals plus melt should be more dense than adjacent or underlying magma and may readily become dislodged by small disturbances (e.g. earthquakes, replenishments to the chamber, and eruptions). The large size of these slurries would ensure rapid settling, even though the weakly attached crystals may disaggregate during downward flow.

ARE MAFIC DYKES FEEDERS FOR THE ENCLAVES?

Numerous syn-plutonic mafic dykes of basaltic composition in the Kameruka Suite plutons indicate migration of mantle-derived melts into and through the pluton as it was crystallizing. Furthermore, the mafic syn-plutonic dykes show all transitions between partial disruption to complete disaggregation as enclave swarms (Collins *et al.*,

Table 4: Nd and Sr isotopic data for the plutonic rocks and dykes

Sample no.	Sample type	$^{87}Sr/^{86}Sr$	Sr (ppm)	Rb (ppm)	$^{87}Rb/^{86}Sr$	$^{87}Sr/^{86}Sr_i$	Nd (ppm)	Sm (ppm)	$^{143}Nd/^{144}Nd$	$^{147}Sm/^{144}Nd$	$^{143}Nd/^{144}Nd_i$	εNd(T)
BH7	adamellite dyke	0·730096	140	203	4·20441	0·70489	7	1	0·512135	0·124998	0·51179	−5·96
BH12	adamellite dyke	0·726706	171	194	3·28965	0·70698	26	5	0·512146	0·107065	0·511851	−4·78
BH25	adamellite dyke	0·735061	116	164	4·10661	0·71044	26	5	0·512165	0·113861	0·511851	−4·78
DB2	Kameruka granodiorite	0·713845	228	113	1·42845	0·70528	28	6	0·512146	0·123831	0·511805	−5·68
DB4	Kameruka granodiorite	0·713039	274	123	1·30185	0·70523	27	5	0·512224	0·116318	0·511903	−3·76
DB6	Kameruka granodiorite	0·712864	272	125	1·32517	0·70492	18	3	0·512259	0·115942	0·511939	−3·05
DB8	Kameruka granodiorite	0·711666	272	115	1·22373	0·70433	16	3	0·512241	0·118109	0·511915	−3·52
BH26	Pericoe adamellite	0·712737	228	101	1·28511	0·70503	42	8	0·512214	0·117103	0·511891	−3·99
BH27	Pericoe adamellite	0·713919	200	97	1·4076	0·70548	36	6	0·512224	0·108382	0·511925	−3·33
DB1	Pericoe adamellite	0·735308	101	230	4·46477	0·70854	18	4	0·512147	0·117363	0·511823	−5·32
DB18	Pericoe adamellite	0·71817	168	141	2·43167	0·70359	59	11	0·512251	0·116476	0·51193	−3·24
DB5	Mafic syn-plutonic dyke	0·704957	299	24	0·23217	0·70356	14	4	0·512665	0·151218	0·512248	2·98
DB7	Mafic syn-plutonic dyke	0·70722	304	78	0·74151	0·70277	15	4	0·512709	0·153156	0·512287	3·73
DB10A	Mafic syn-plutonic dyke	0·70591	340	48	0·23219	0·70452	14	3	0·512707	0·147845	0·512299	3·98

For εNd calc., $^{143}Nd/^{144}Nd$ CHUR = 0·512638; $^{147}Sm/^{144}Nd$ today = 0·1967.

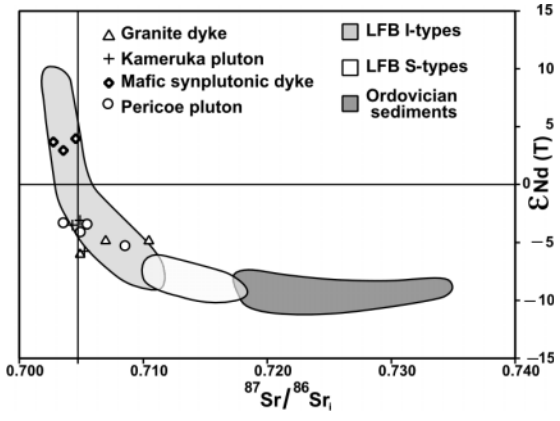

Fig. 13. Plot of εNd(T) vs Sr(i) for the Kameruka Suite samples compared with the Lachlan Fold Belt (LFB) I- and S-type granites and Ordovician sediments (from McCulloch & Chappell, 1982; B. Healy, unpublished data).

2000*a*, fig. 5). Enclaves within these syn-plutonic dykes show exactly the same features as enclaves dispersed throughout the granite. For example, one of the aforementioned dykes contains xenocryst-poor mafic enclaves in a xenocryst-rich tonalitic host (Collins *et al.*, 2000*a*; fig. 4e and f), similar to the enclave–matrix relations of the Illawambra enclave swarm (Fig. 3). In some other plutons, composite dykes can be seen to connect with (and hence apparently feed) layers of enclaves and their enclosing granitic mush (Wiebe *et al.*, 2002). To contain abundant K-feldspar xenocrysts, the dykes must have intruded through crystal-rich mush and entrained crystals from this host. These dense mafic replenishments probably rolled across the aggrading chamber floor, producing complex mixing zones characterized by xenocryst-rich hybrids that are host to more mafic enclaves, as at Illawambra Weir. These features are consistent with a cumulate model suggesting that granitic magma chambers build upward by floor aggradation (see Wiebe & Collins, 1998).

Enclave samples from the abovementioned mafic syn-plutonic dykes form part of the geochemical array of Fig. 12, and confirm the intimate relation between mantle melts and enclave compositions. However, the basalts generally do not lie on the granite–enclave trends, implying modification of the basaltic melts before incorporation as enclaves in the granite. In particular, the marked decrease in MgO (and Ni), and increase in Al_2O_3, Na_2O and Sr, are typical of features associated with two-pyroxene fractionation of hydrous arc basalts in the deep crust (Müntener *et al.*, 2001). Shallow-level fractionation (upper crustal) involving plagioclase does not produce elevated Al_2O_3 and Na_2O contents (Grove *et al.*, 2003). The spiked trace element patterns of these basalts, particularly the positive Sr and negative Nb anomalies, and the dominance of magmatic hornblende, strongly support a hydrous arc magma origin (Collins, 2002). Thus, the sub-linear trends of the enclaves, which extrapolate to high Al_2O_3, Na_2O and Sr, but low MgO and Ni at the basaltic end (Fig. 12), indicate that the basaltic magmas had fractionated in the deep crust before hybridization and incorporation in the granitic magma chamber.

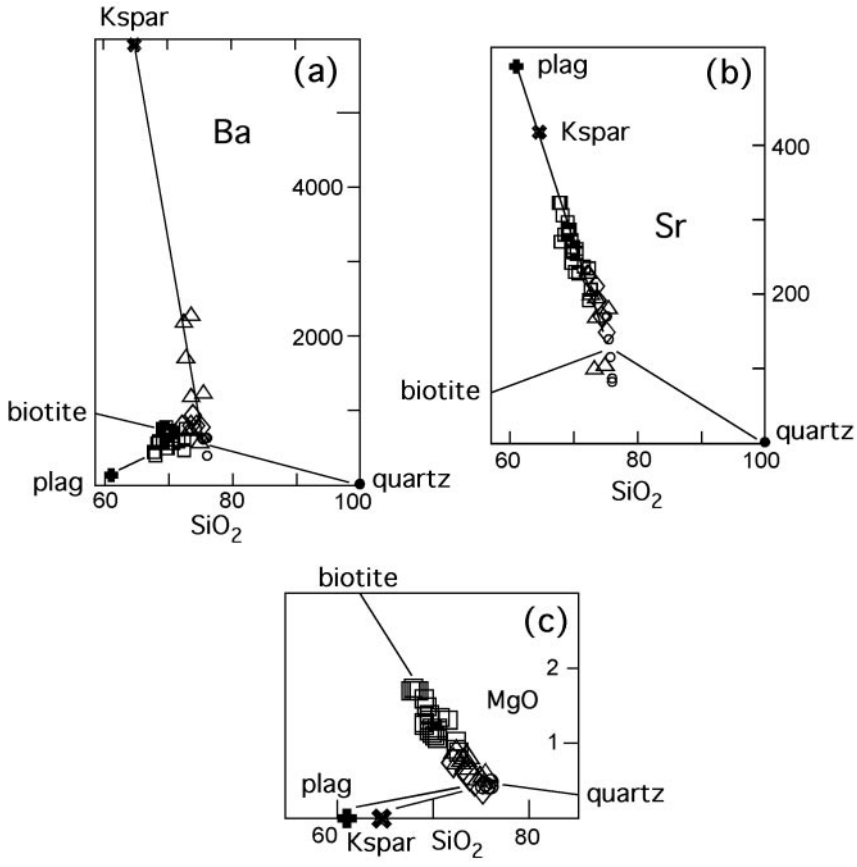

Fig. 14. Variation of Ba (a), Sr (b) and MgO (c) vs wt % SiO_2 for Kameruka Suite granites and minerals from a representative granodiorite (KSS-5C) in the Kameruka pluton. Symbols are as for Fig. 11. The projection of whole-rock samples consistently through a line between minerals and dykes indicates that the mineral compositions are representative. (See text for explanation.)

The widespread occurrence of large corroded crystals of alkali feldspar and quartz within intermediate enclaves that have fine-grained igneous textures indicates that these enclaves reflect either mixing between resident silicic crystal mushes and replenishments of mafic magma (Wiebe, 1993) or mechanical incorporation (plucking) of crystals from the crystal-rich, host granite mush by hybridized syn-magmatic dykes, which were subsequently dispersed into the melt-rich portion of the magma chamber (Collins *et al.*, 2000*a*). The prominent biotite in the common enclaves is likely to reflect selective exchange of alkalis and water with the enclosing granite, as has been commonly noted in many occurrences of commingled mafic and silicic magmas (Wiebe, 1973). The presence of basaltic to andesitic, syn-plutonic dykes in the Kameruka pluton provides independent evidence for replenishment by mafic–intermediate magmas, and all stages of dismemberment of these syn-magmatic dykes, via enclave swarms and dispersed enclave trains, have been documented in the pluton (Collins *et al.*, 2000*a*).

ARE GRANITIC DYKES FEEDERS FOR THE PLUTONS?

Silicic dykes, with textures and compositions suggesting that they were crystal-poor liquids when emplaced, occur widely throughout the Kameruka Suite plutons. They are most common at or below the pluton base (Collins *et al.*, 2000*a*, 2000*b*), but smaller dykes of comparable composition occur within a few kilometres of the eastern (upper) margin of the intrusion. The large thickness of some dykes (up to 30 m) suggests that they could have transported large volumes of granitic magma (e.g. Clemens & Mawer, 1992; Petford *et al.*, 2000). The microgranite dyke described in the Towamba River (Fig. 6), which has a composition similar to that of the large dykes, can be traced from below the pluton to a zone where it spread laterally and formed a diffuse semi-concordant sheet. These gradational contacts demonstrate that the dyke was emplaced into semi-consolidated granitic material of the porphyritic Kameruka granodiorite, and was a feeder dyke to that pluton.

It is possible that the felsic dykes are differentiates from another pluton located at greater depth. However, their equigranular, non-porphyritic nature suggests that they were not extracted from any crystallizing magma chamber, and gravity surveys across the suite in several locations replicate the inferred depth of the pluton, based on field constraints (Richards & Collins, 2004). As such, deeper plutonic bodies are probably not present. Also, it is highly unlikely that syn-plutonic basaltic dykes, which locally share the same pathways as the felsic dykes, could have traversed through a deeper molten body. The field, petrographic and geophysical evidence favours an origin for these dykes as feeders directly from the source region (e.g. Clemens & Mawer, 1992).

Some hornblende-bearing, intermediate composition dykes (53–67% SiO_2) have intruded the base of the Kameruka pluton in the Towamba River basin (Collins *et al.*, 2000*a*; Fig. 1, locality 1). These dykes represent hybrids between the basaltic and granitic dykes, and indicate that the dyke magmas were interacting with mafic magmas at depth. This reinforces a deep-seated origin for all the dykes. Also, the dykes broadly fall along the extrapolation of the Kameruka Suite chemical trends (Collins *et al.*, 2000*a*; Fig. 6), which indicates that they could have contributed to magma diversity in the pluton. However, the paucity of these dykes, the lack of hornblende in the pluton, and the separate isotopic cluster for that suite suggest that the input from these intermediate dykes was minimal.

The chemical compositions of the felsic dykes lie at the SiO_2-rich end of compositional trends of the granitic plutons. Their major element compositions closely match some analysed granodiorites near the base of the Kameruka pluton, differing mainly in having lower concentrations of Fe, Mg and Ca than the granodiorite (e.g. compare KSS-7A with dykes in Table 2). Trace element concentrations in the cores of early crystallizing minerals (sample KSS-5C), with few exceptions, are consistent with the range of expected partition coefficients (Table 5), suggesting that the dykes were parental to the granites of the pluton. This possibility can be checked independently by calculating the specific partition coefficient for plagioclase, using the equations of Blundy & Wood (1991). For the least evolved felsic dyke (BH12), which contains inherited zircon cores, a zircon saturation temperature of 762°C was calculated (Watson & Harrison, 1983). At this temperature, the measured partition coefficient for plagioclase of An_{40} is 6·5 for Sr and 0·55 for Ba, slightly higher than the values shown in Table 5. For plagioclase of An_{50}, values of ~4·3 for Sr and ~0·3 for Ba are obtained, which are a better approximation to those of Table 5, suggesting that we have not analysed the most calcic cores in the dykes. Therefore, in spite of likely effects of fractionation and some contamination by mafic magmas, the trace element data from plagioclase in the pluton are consistent with derivation by crystallization from the felsic dykes.

Taking the average composition of these dykes, we used a least-squares approximation of the major elements (Bryan *et al.*, 1969) to test whether or not the large dykes below the intrusion in the Towamba River basin could represent appropriate parental liquids to produce rocks having the compositions of typical Pericoe granitic rocks above them. Using major element compositions in minerals from specimen KSS-5A, regressions produce excellent matches with low residuals (Table 6). They require accumulation of reasonable amounts and proportions of early-forming minerals (plagioclase, quartz, K-feldspar, biotite, and apatite), with the calculated amount of trapped dyke liquid ranging from about 70 to 30%. The apparent amount of trapped melt is larger toward the base of the body; which may reflect more rapid aggradation of the chamber floor in the early stages of magma emplacement.

IMPLICATIONS FOR OPEN-SYSTEM CRYSTALLIZATION OF THE KAMERUKA MAGMA CHAMBER

The presence of many felsic and fewer mafic feeder dykes, and dispersed enclave swarms, indicates that the magma chamber that produced the Kameruka Suite was an open system in terms of renewed magmatic input. In this respect, it resembles replenished magma chambers often inferred from studies of erupted rocks (Bacon, 1983; Eichelberger *et al.*, 2000). Because of the widespread evidence for crystal deposition and because typical samples of the granite appear to have accumulated between about 30 and 70% crystals, the bulk composition of the Kameruka granodiorite cannot represent the liquid or magma emplaced. The total composition of the exposed parts of the pluton must, therefore, be enriched in crystals relative to any silicic parental magma.

Replenishments to and eruptions from a magma chamber can have important implications for the compositional evolution of magmas in that chamber, and for the resulting compositional variation of the cumulates that form from those magmas. Magma compositions in the chamber need not evolve through time in a unidirectional way, but could vary back and forth as replenishments (felsic and mafic) occur. Replenishments may also cause the magma chamber to be compositionally stratified in different ways and at different times. If silicic dykes of similar composition regularly feed a magma chamber that is both accumulating crystals on the chamber floor and erupting more evolved melts from its roof, the average composition of magma in the chamber and the minerals that accumulate on the

Table 5: Comparison of published mineral–melt partition coefficients (Rollinson, 1993) with values calculated using the ratio of trace element concentrations in the cores of cumulate minerals (specimen KSS-5C) to the average concentrations in fine-grained granitic dykes (Table 2)

	BH24 granitic dyke	BH1 granitic dyke	BH7 granitic dyke	BH12 granitic dyke	BH25 granitic dyke	average granitic dyke
SiO_2	75·45	75·28	74·96	74·6	75·45	75·15
TiO_2	0·19	0·17	0·19	0·19	0·21	0·19
Al_2O_3	13·11	13·39	13·32	13·51	13·29	13·32
Fe_2O_3	1·14	1·37	1·58	1·61	1·29	1·40
FeO	0·00	0·00	0·00	0·00	0·00	0·00
MnO	0·01	0·03	0·03	0·03	0·01	0·02
MgO	0·42	0·49	0·44	0·41	0·41	0·43
CaO	0·9	0·7	1·27	1·35	1·19	1·08
Na_2O	2·53	2·99	3·02	3·21	2·83	2·92
K_2O	5·13	4·37	4·27	3·99	4·45	4·44
P_2O_5	0·09	0·06	0·06	0·05	0·08	0·07
LOI	0·73	0·95	0·6	0·7	0·86	0·77
Total	99·71	99·77	99·72	99·65	100·05	99·78
Ba	620	385·5	609·5	619·5	627	572
Rb	189	184·5	203	193·5	163·5	187
Sr	82	87·5	140	170·5	115·5	119
Pb	38	42·5	31·5	33·5	37	37
Th	10	21	24	28·5	22·5	21
U	5	2	2	2	2	3
Zr	98	78	102·5	108	119	101
Nb	2	2	2	6	5	3
Y	16	21	19·5	21	23·5	20
La	22	22·5	27	16·5	24·5	23
Ce	36	35·5	59	49·5	46·5	45
Nd						
Sc						
V	1	9·5	22	14	14	12
Cr	2	2	2	2	2	2
Co	100	115	73·5	108	102·5	100
Ni	1	1	1	1	1	1
Cu	1	1	1	1	1	1
Zn	20	16	26	21	18·5	20
Ga	14	22	23	28	23	22

	KSS-5C plag	kspar	biotite	apatite	Av. dyke	apparent K_d plag	kspar	biotite	apatite
Ba	146	5920	1457	4	572	0·26	10·34	2·54	0·01
Rb	3	306	766	1	187	0·02	1·64	4·10	0·01
Sr	508	419	1	176	119	4·27	3·52	0·01	1·48
Pb	21·3	54·0	3	6	37	0·58	1·48	0·08	0·17
Nb			82	0	3			27·17	
Y			0	2860	20	0·00	0·00	0·00	141·58
La	16·1	1·8	0	327	23	0·72	0·08	0·02	14·52
Ce	23·3	1·5	1	1150	45	0·52	0·03	0·01	25·38
V			417	1	12			34·71	
Co			44	0	100			0·44	
Ga	28	108	67	1	22	1·28	4·91	3·02	0·05

plag K_d values	Rollinson	Henderson	calc.
Ba	0·3–1·5	0·3–0·9	0·26
Rb	0·04–0·1	0·02–0·46	0·02
Sr	3–16	1·5–8·8	4·27
Pb	0·97	0·3–0·8	0·58
La	0·38	0·24–0·49	0·72

biotite K_d values	Rollinson	Henderson	calc.
Ba	5·4–23·5	6·4–8·7	2·54
Rb	2·2–4·2	3·3–3·5	4·10
Sr	0·2–0·45	0·12–0·36	0·01
Nb			27·17
La		0·32	0·02
Ce	0·04–0·32	0·04–0·38	0·01

apatite K_d values	Rollinson	Henderson	calc.
Y	40·00		141·58
La	14·50		14·52
Ce	21–35	17–53	25·38

Kspar K_d values	Rollinson	Henderson	calc.
		2·7–12·9	10·34
	0·3–1·8	0·11–0·8	1·64
	3·8–5·4	3·6–26	3·52
	2·50	0·84–1·4	1·48
	0·08		0·08

chamber floor may remain roughly constant. In the Kameruka pluton, large crystals of plagioclase, quartz and biotite, in broadly similar proportions, are present in all rocks at all levels of the intrusion, consistent with replenishment by silicic magma of uniform composition. Even if the melt changes, it must change enough to reach saturation in a new phase or become undersaturated in an existing cumulus mineral, in order to change the composition of the accumulating material strongly.

The irregular occurrence and variable reaction shown by alkali feldspar megacrysts in the Kameruka pluton suggest that mafic and felsic replenishments through time frequently caused the resident magma to leave the stability field of alkali feldspar. Those megacrysts

Table 6: Least-squares modelling of major elements (Bryan et al.*, 1969) to test whether or not the large dykes below the intrusion in the Towamba River basin could represent appropriate parental liquids to produce rocks having the compositions of the typical Pericoe granitic rocks above them*

Height above base:	lowest				highest
	DB-1	DB-9	DB-18	BH-26	BH-27
% dyke liquid	69·7	57·6	73·4	27·8	37·9
% plagioclase	9·7	11·0	11·7	32·0	26·5
% K-feldspar	6·5	10·0	1·3	5·8	7·1
% quartz	8·5	17·2	8·0	25·1	20·6
% biotite	5·4	4·0	5·4	9·1	7·7
% apatite	0·2	0·2	0·2	0·2	0·2
	100·0	100·0	100·0	100·0	100·0
Solids					
% plagioclase	32·0	25·7	44·1	44·3	42·6
% K-feldspar	21·5	23·5	4·9	8·0	11·4
% quartz	28·0	40·8	30·1	34·8	33·3
% biotite	17·8	9·6	20·3	12·6	12·4
% apatite	0·7	0·5	0·6	0·3	0·3
	100·0	100·0	100·0	100·0	100·0
Sum of squares of the residuals	0·011	0·004	0·012	0·014	0·015

Based on the average of the five fine-grained granitic dykes (Table 2) and the mineral compositions of KSS-5C (Table 1).

without plagioclase reaction rims occur mainly in the lower parts of the intrusion, where they are euhedral, but at higher levels such feldspars are erratic in abundance and distribution. At these higher levels, most megacrysts are rounded and have plagioclase rims of varying thickness (Fig. 9a), indicating that alkali feldspar was then not crystallizing from the enclosing magma, but, rather, was reacting with it. Replenishments of new silicic magma and, particularly, hotter, mafic input marked by swarms of mafic inclusions (e.g. the Bega River and Illawambra swarms) may have shifted the composition of magma near the base of the chamber away from saturation in alkali feldspar. None the less, alkali feldspar may have continued to crystallize at higher levels in the magma chamber, perhaps reflecting compositional stratification. If slurries from the upper part of the chamber sank toward the floor, alkali feldspar would have been out of equilibrium with magma in the lower parts of the chamber, leading to the development of plagioclase reaction rims. Thus, within adjacent grains of any sample, variable growth and resorption of alkali feldspar is an excellent record of convective movement of magma and open-system behaviour in the magma chamber that produced the Kameruka pluton.

According to an open-system model, fractionated products should be present in the upper portions of the pluton, but they are not generally present in the Kameruka Suite. They could represent the locally extensive bodies of microgranite within the suite, or the melts could have been evacuated during successive mafic replenishments, to erupt as volcanics. In the northern Bega Batholith, comagmatic volcanics exist (Wyborn & Chappell, 1986; Wyborn & Owen, 1986), and elsewhere in the Lachlan Fold Belt, extrusive volcanic units also can be directly related to their plutonic counterparts (e.g. Wyborn *et al.*, 1981; Simpson, 1986). However, such roof-related volcanics are absent in the southern Bega Batholith. In the study area, the floor of the pluton is observed (Fig. 4), and P–T conditions suggest ~3 kbar (10 km) depth (Richards & Collins, 2004), so it is unlikely that we have sampled the fractionated melt products in this study.

The floor aggradation model (Wiebe & Collins, 1998) implies that the amount of magma present at any one time is minimal, perhaps only a 'layer' several hundred metres thick at the top of the chamber. This is consistent with seismic tomography studies of active silicic volcanoes, which rarely show a large upper crustal magma chamber beneath them (e.g. Iyer *et al.*, 1990). Such a thin film, at least several hundred metres thick if explanations for the Candelo tonalite raft (Fig. 7) are correct, would mix with felsic replenishments and the composition would be continually buffered, so the chamber might not fractionate significantly. More

importantly, if a fractionated magma remains during the final stages of pluton construction, it will not be of large volume, and could easily be represented by rhyolitic horizons in the volcanic successions located to the north. We have yet to test this possibility.

THE ORIGIN OF CHEMICAL VARIATION IN THE KAMERUKA SUITE

Chemical analyses of samples from the Kameruka, Illawambra and Pericoe plutons plus associated fine-grained granitic dykes, yield essentially linear, though scattered, trends for most elements on Harker diagrams, with SiO_2 ranging from about 67 to 76 wt % (Fig. 10). The fine-grained granitic dykes have the highest SiO_2 contents and the Kameruka pluton the lowest. Because Chappell (1996*a*, 1996*b*) has previously noted these linear trends for the Kameruka pluton and suggested that they could only have been caused by restite unmixing, rather than either magma mixing (Reid & Hamilton, 1987) or fractional crystallization (Wall *et al.*, 1987), it is necessary to consider why these other processes cannot be the dominant explanation for the variation in these plutons. We briefly review these three options separately, though recognizing that all three processes, and others (e.g. assimilation), may contribute to compositional variation.

Magma mixing models imply that chemical variation develops either by mixing of different proportions of contrasted end-members, or by fractional crystallization of a hybridized parental magma. Mixing models require open-system behaviour in which the end-member source composition cannot be confidently ascertained, as rock compositions could be modified by either fractional crystallization or crystal accumulation. For granitic systems, most of these models are based mainly on theoretical, experimental and geochemical considerations. If magma mixing is the cause of linear compositional trends, thorough bulk mixing between compositionally distinct end-members (mafic and silicic) must occur. There are physical barriers that must be overcome to accomplish chamber-scale mixing (Sparks & Marshall, 1986; Campbell & Turner, 1986; Frost & Mahood, 1987), and the linear trends could readily be destroyed if the mixed magma crystallized to produce cumulates and more evolved liquids.

Systematic differences in linear chemical variations between the super-suites of the Bega Batholith have been used by Chappell (1996*a*, 1996*b*) to argue against magma mixing models. Chappell noted that the chemical character (e.g. high Sr) at the mafic end of the compositional spectrum is generally also observed at the felsic end for each suite or super-suite, which is an argument against simple magma mixing as the cause of compositional variation. Independently, Nd–Sr isotopic data (Table 4) show no systematic variation in $^{87}Sr/^{86}Sr_i$ or εNd with varying SiO_2 in the various units (plutons or dykes) of the Kameruka Suite. Thus, we also conclude that magma mixing cannot have produced the near-linear compositional variations in the Kameruka Suite, but it may have produced discrete compositional batches represented by the separate plutonic phases.

The presence of numerous mafic enclaves indicates that mafic magmas were present and could have mixed with Kameruka magmas, particularly as petrographic and geochemical data demonstrate that the enclaves are hybrid in origin. The most mafic enclaves (~55 wt % SiO_2) were probably basalts that fractionated at high pressure before incorporation in the granitic magma chamber (see above), and the projections to the most mafic Kamuruka granites (~67 wt % SiO_2) for some elements, such as FeO, CaO and Al_2O_3 (Fig. 12a), imply mixing. However, the enclave scatter in TiO_2, P_2O_5, MgO, Sr and Zr, compared with the tight array defined by the granites (Fig. 12), seems to militate against this possibility, although variable addition of minerals from the granitic mush, and possibly late magmatic to subsolidus diffusion, would contribute to this dispersion. The small isotopic shifts of the Kameruka plutons along the Sr–Nd array, between the mafic and felsic dykes (Fig. 13), does suggest that some mafic material has been mixed into the Kameruka magma. Perhaps discrete mixing events generated these shifts, but the bulk composition of the granitic magma was buffered by a crystallizing assemblage that was established early in the history of pluton construction and did not change with successive replenishments (Fig. 14). This possibility favours a cumulate model for producing the chemical variation, as discussed below.

The restite unmixing model assumes that chemical variation reflects closed-system removal of restitic components from a compositionally uniform felsic melt and that the source material was compositionally similar to, or the chemical image of, the most mafic analysed granitic rock in the suite. Granites of the Lachlan Fold Belt, including the suites of the Bega Batholith, are the type examples for restite unmixing (Chappell *et al.*, 1987; White & Chappell, 1977; Griffin *et al.*, 1978; Hine *et al.*, 1978), where it has been argued that well-defined linear variation trends must result from that process. The restite model suggests that, during partial melting, the source melts to form a felsic liquid and a solid restitic framework. At an assumed critical melt fraction of ~25–30%, the melt rises buoyantly and breaks the framework, diapirically raising the source *en masse* to higher crustal levels. According to this model, progressive separation of restite from the melt produces the linear chemical variation.

Using the criteria of Chappell *et al.* (1987), we see no convincing textural evidence for a significant amount of restite in these plutons. Plagioclase shows weak normal and oscillatory zoning and any Ca-rich (possibly 'restitic') cores are rare. Those present could well have originated by mixing of minerals from the observed mafic input. Although it is true that inherited cores of zircons do occur (Paterson *et al.*, 1992), they represent a miniscule part of the mineral assemblage and variation in their abundance cannot explain the compositional variation of the plutons. Also, ragged mafic mineral aggregates are restricted to the hybrid tonalitic phases that form the matrix to the enclave swarms (e.g. Illawambra). The only major mafic mineral is biotite, which mainly occurs as discrete flakes in interstices between the larger quartz–feldspar grains (Fig. 9). An interpretation that individual biotite grains were trapped in a cumulate framework of felsic minerals, rather than representing restite, is much more consistent with the textural relations. The field evidence that very fine-grained, phenocryst-poor silicic dykes have intruded into the magma chamber from below and have replenished the plutonic system, is also not consistent with retention of significant amounts of restite during ascent of the magma.

Restite unmixing could produce the linear trends on Harker diagrams, but this model cannot explain the Ba vs SiO_2 trend, for example. Along with decreasing Zr, increasing Ba in the 65–75 wt % silica range (Fig. 12b) is a hallmark signature of typical 'low-temperature' granites (Chappell *et al.*, 1998, p. 234), consistent with progressive removal of a biotite- and plagioclase-dominated restite from a melt of near-constant haplogranite composition. In the restite model, Ba concentration should be constant in the felsic melt. Thus, the marked Ba spike for the Pericoe pluton (Fig. 10b), which is defined by the melt–K-feldspar tie-line (Fig. 14), is anomalous; a similar spike exists for La (and Ce and Zr to a lesser extent). The strong negative correlations with SiO_2 are better explained by K-feldspar, zircon and probably allanite forming as cumulus phases that have concentrated in the Pericoe pluton. This interpretation might seem at odds with the presence of large K-feldspar megacrysts in the Kameruka pluton, but the granodioritic composition of that pluton indicates that, although conspicuous, they are not abundant. Ba variation in the Kameruka Suite strongly suggests that chemical variation has evolved from high to low silica as cumulates have progressively formed, not from low to high silica with restite removal. Ba variation is consistent with the field interpretation that the felsic dykes contained the primary granitic melts.

Field, petrographic, and chemical evidence indicates that the Kameruka pluton is a cumulate (stratigraphic) sequence that youngs to the east. The presence of multiple felsic and mafic dykes with appropriate compositions for feeders, and the lack of systematic variation to more evolved compositions with stratigraphic level, provide strong evidence for an open system that was multiply replenished. Nd–Sr isotopic variation indicates that some mixing (possibly highly selective) between mafic and felsic magma has occurred. A fundamental question is whether a pluton produced by these processes can generate sublinear compositional trends on Harker variation diagrams.

In rejecting fractional crystallization models for the Bega Batholith, Chappell (1996*b*) assumed closed-system fractionation and a constant ~3:1 ratio of cumulus mineral to trapped melt over the entire silica range of each studied suite. He also used changing modal proportions to assert that mineral–liquid partition coefficents of Ba and Sr should change significantly during fractionation, and concluded that fractionation should produce curved rather than the observed linear variation trends. The assertion that mineral–liquid partition coefficients must change during fractionation is conditional on closed-system behaviour. If the system is open, as we show the Kameruka pluton must have been, the mineral–liquid partition coefficents need not change significantly throughout crystallization, and the chemical trends may be sublinear.

None the less, open-system fractionation and formation of cumulates should produce curved trends for the most strongly compatible or incompatible elements. However, elements such as Ni and Cr are too low or scattered over the 67–76 wt % SiO_2 range to provide definitive evidence. It is possible that the Rb and Pb trends are curved upward, and the Sr and Zr trends curved downward (Fig. 12), but this is tenuous, again because of elemental scatter. The data highlight the equivocal petrological interpretations that derive from reliance on selected sublinear trends on Harker diagrams.

The cumulate control of compositional variation becomes clearer when one focuses on variation within individual plutons. Tie-lines from the fine-grained dykes (liquids) to selected trace and major element compositions of the cores of cumulus minerals are plotted in Harker diagrams along with the whole-rock compositions of the granites (Fig. 14). The Kameruka, Illawambra and Pericoe plutons all lie along a single line from liquid to biotite in a plot of MgO vs SiO_2 and from liquid to plagioclase and K-feldspar in a plot of Sr vs SiO_2. No other early crystallizing phases have significant concentrations of these elements, so compositional variation can be readily explained by fractional crystallization of these minerals.

A cumulate model explains the divergent trend of Zr for the different plutonic phases, as well as the presence of inherited zircon, and the 'low-temperature' status of

the Kameruka Suite. The two trends of Zr, divergent from high to low SiO_2 (Fig. 12b), are a subdued version of the Ba trend, and consistent with zircon accumulation in magmas of different initial Zr concentrations. The restite model would require an impossibly Zr-, Ba- and light rare earth element (LREE)-rich source for the Pericoe pluton to explain the spikes in these elements (Fig. 12), yet field evidence shows that the pluton is intimately related to the Kameruka pluton and derived from the same magma. Like all the plutonic phases, the felsic dykes contain inherited zircon, indicating that it was incompletely dissolved during the production of the 'low-temperature' silicic melt. These cores were coated with Zr from the melt during crystallization and were eventually incorporated into the cumulate, commonly within grains of interstitial biotite. Thus, the melt composition and zircon inheritance are explicable by a restite unmixing model, but the subtleties of Zr (and Ba, La, Ce) variation, and the textural evidence, are much better accommodated by a cumulate model.

A cumulate model also can explain Chappell's observation that the high- and low-SiO_2 end of the granite suites of the Bega Batholith share the same distinctive chemical character; that is, both ends share relatively high or low concentrations of certain trace elements. The trace element concentrations in cumulates reflect the abundance of those elements in the liquid and the bulk partition coefficients of the cumulus mineral assemblage. For example, Sr-rich silicic liquids should produce Sr-rich cumulus feldspar, so the linear cumulate trend will project to high Sr at the low-SiO_2 end of the trend. In contrast, Sr-poor granitic liquids will generate Sr-poor trends. This is the same approach as used to explain the strong negative trend of Ba vs SiO_2 in the Pericoe pluton. In other words, the original chemistry of the parental liquid is imparted onto the cumulus mineral assemblages (the granites of the suite). A major implication is that the sampled granites of the Bega Batholith could all be cumulates. The cumulate model provides an explanation of why the SiO_2-rich end 'sees' the SiO_2-poor end of the super-suite compositional trend in the Bega Batholith.

CONCLUSIONS: CONSTRUCTION OF THE KAMERUKA INTRUSION

Based on the field, petrographic and chemical evidence outlined above, the following conclusions may be reached.

(1) The Kameruka magma chamber was fed by crystal-poor magmas that were transported by dykes. The presence of ubiquitous mafic enclaves throughout the pluton and a subtle isotopic shift away from the average silicic dyke composition toward the mafic dyke compositions indicate that mixing of end-member components was minor.

(2) The Kameruka pluton solidified largely by crystal accumulation on the chamber floor that has a regional eastward tilt. Depositional features include enclave channels, subparallel swarms containing asymmetric (pillow-shaped) enclaves exhibiting chilled bases and hybrid tops, mafic layers also exhibiting pillow-structures, load casts and flame structures, preferential compaction of granitic mush on the western (lower) side of enclaves, trough cross-beds, and large stoped blocks that apparently fractured the chamber floor and themselves during impact. As such, the Kameruka pluton preserves a stratigraphic record of its construction.

(3) The magma chamber was an open system—replenished by silicic magmas and periodically invaded by mafic magmas. The dominance of dykes (silicic, mafic and composite) near the base, some of which have transitional contacts with the pluton at higher levels, indicates open-system behaviour. No evidence exists for *en masse* movement and diapiric emplacement of magma.

(4) The closed-system restite model cannot explain the field and textural relations of the Kameruka Suite of plutons, and restite unmixing is not a unique solution for the observed linear chemical trends.

(5) The range of chemical variation and major element modelling is consistent with a cumulate, open-system model, whereby replenishment by silicic magmas buffered the composition of the fractionating magma chamber. As a result, the crystallizing mineral assemblage did not change and accumulation of precipitating minerals in different proportions produced linear chemical variation trends.

(6) A cumulate model can explain the enigmatic chemical trends of the Bega Batholith, where the high- and low-SiO_2 end-members of the granite suite contain high concentrations of particular trace elements. This simply reflects accumulation of crystals that formed in a silicic magma chamber with high initial concentrations of those elements.

ACKNOWLEDGEMENTS

This work was supported by ARC Grant A00103. We thank Ian Campbell, and Tony Kemp in particular, for thoughtful comments and review. Early studies by Honours students (D. Barrett, M. Brocklesby and P. Ellison) helped provide the framework for this study.

SUPPLEMENTARY DATA

Supplementary data for this paper are available at *Journal of Petrology* online.

REFERENCES

Bacon, C. R. (1983). Eruptive history of Mount Mazama and Crater Lake Caldera, Cascade Range, USA. *Journal of Volcanology and Geothermal Research* **18**, 57–115.

Baker, D. R. (1998). Granitic melt viscosity and formation. *Journal of Structural Geology* **20**, 1395–1404.

Barrett, D. (1998). Causes of chemical variation in Kameruka Supersuite plutons, Bega Batholith, New South Wales. B.Sc. Hons thesis, University of Newcastle, Newcastle, Australia.

Bartlett, R. W. (1969). Magma convection, temperature distribution, and differentiation. *American Journal of Science* **267**, 1067–1082.

Beams, S. D. (1980). Magmatic evolution of the southeast Lachlan Fold Belt, Australia. Ph.D. thesis. La Trobe University, Victoria, Australia.

Bennett, V. C., Nutman, A. P. & McCulloch, M. T. (1993). Nd isotopic evidence for transient, highly depleted mantle reservoirs in the early history of the Earth. *Earth and Planetary Science Letters* **119**, 299–317.

Blundy, J. D. & Wood, B. J. (1991). Crystal-chemical controls on the partitioning of Sr and Ba between plagioclase feldspar, silicate melts, and hydrothermal solutions. *Geochimica et Cosmochimica Acta* **55**, 193–209.

Bryan, W. B., Finger, L. W. & Chayes, F. (1969). Estimating proportions in petrographic mixing equations by least squares approximation. *Science* **163**, 926–927.

Campbell, I. H. (1978). Some problems with the cumulus theory. *Lithos* **11**, 311–323.

Campbell, I. H. & Turner, J. S. (1986). The influence of viscosity on fountains in magma chambers. *Journal of Petrology* **27**, 1–30.

Chappell, B. W. (1996*a*). Magma mixing and the production of compositional variation within granite suites: evidence from the granites of southeastern Australia. *Journal of Petrology* **37**, 449–470.

Chappell, B. W. (1996*b*). Compositional variation within granite suites of the Lachlan Fold Belt: its causes and implications for the physical state of granitoid magmas. *Transactions of the Royal Society of Edinburgh* **87**, 159–170.

Chappell, B. W., White, A. J. R. & Wyborn, D. (1987). The importance of residual source material (restite) in granite petrogenesis. *Journal of Petrology* **28**, 1111–1138.

Chappell, B. W., White, A. J. R. & Williams, I. S. (1991). A transverse section through granites of the Lachlan Fold Belt: Second Hutton Symposium Excursion Guide. *Bureau of Mineral Resources, Geology and Geophysics, Canberra, Record* **1991/22**, 125 pp.

Chappell, B. W., Bryant, C. J., Wyborn, D., White, A. J. R. & Williams, I. S. (1998). High- and low-temperature granites. *Resource Geology* **48**, 225–236.

Clemens, J. D. & Mawer, C. K. (1992). Granitic magma transport by fracture propagation. *Tectonophysics* **204**, 339–360.

Collins, W. J. (2002). Nature of extensional accretionary orogens. *Tectonics* **21**, 1258–1272, doi:10.1029/2000TC001272.

Collins, W. J., Richards, S. W., Healy, B. & Ellison, P. I. (2000*a*). Origin of heterogeneous mafic enclaves by two-stage hybridisation in magma conduits (dykes) and below and in granitic magma chambers. *Transactions of the Royal Society of Edinburgh* **91**, 27–45.

Collins, W. J., Richards, S. W., Healy, B. & Wiebe, R. A. (2000*b*). Granite magma transfer, pluton construction, the role of coeval mafic magmas, and the metamorphic response: southeastern. *Lachlan Fold Belt, FP3*. Sydney: Geological Society of Australia Incorporated, 153 pp.

Eichelberger, J. C., Chertkoff, D. G., Dreher, S. T. & Nye, C. J. (2000). Magmas in collision: rethinking chemical zonation in silicic magmas. *Geology* **28**, 603–606.

Ellison, P. I. (1999). The emplacement and deposition of mafic enclaves: the Kameruka Supersuite. B.Sc. Hons thesis, University of Newcastle, Newcastle, Australia.

Emeleus, C. H. (1963). Structural and petrographic observations on layered granites from southern Greenland. *Mineralogical Society of America, Special Paper* **1**, 22–29 In: Fisher, D.J., Frueh, A.J., Hurlbut, C.S., Jr & Tilley, C.E. (1963) (eds) *Papers and Proceedings of the Third General Meeting*, Washington, D.C., April 17-20, 1962.

Frost, T. P. & Mahood, G. A. (1987). Field, chemical and physical constraints on mafic–felsic magma interaction in the Lamark Granodiorite, Sierra Nevada, California. *Geological Society of America Bulletin* **99**, 272–291.

Gilbert, G. K. (1906). Gravitational assemblage in granite. *Geological Society of America Bulletin* **17**, 321–328.

Griffin, T. J., White, A. J. R. & Chappell, B. W. (1978). The Moruya Batholith and geochemical contrasts between the Moruya and Jindabyne suites. *Journal of the Geological Society of Australia* **25**, 235–247.

Grove, T. L., Elkins-Tanton, L. T., Parman, S. W., Chatterjee, N., Müntener, O. & Gaetani, G. A. (2003). Fractional crystallization and mantle-melting controls on calc-alkaline differentiation trends. *Contributions to Mineralogy and Petrology* **145**, 515–533.

Hibbard, M. J. (1991). Textural anatomy of twelve magma-mixed granitoid systems., In: Didier, J. & Barbarin, B. (1991). *Enclaves and Granite Petrology*, Amsterdam: Elsevier, pp. 158-170.

Hine, R. H., Williams, I. S., Chappell, B. W. & White, A. J. R. (1978). Geochemical contrasts between I- and S-type granitoids of the Koskiusko Batholith. *Journal of the Geological Society of Australia* **25**, 215–234.

Irvine, T. N. (1974). *Petrology of the Duke Island Ultramafic Complex, Southeastern Alaska. Geological Society of America, Memoirs* **138**, 240 pp.

Irvine, T. N. (1982). Terminology for layered intrusions. *Journal of Petrology* **23**, 127–162.

Iyer, H. M., Evans, J. R., Dawson, P. B., Stauber, D. A. & Acheuer, U. (1990). Differences in magma storage in different volcanic environments as revealed by seismic tomography: silicic volcanic centres and subduction-related volcanoes. In: Ryan, M. P. (ed.) *Magma Transport and Storage*. Chichester: John Wiley, pp. 293–316.

Jackson, S. E. (2001). The application of Nd:YAG lasers in LA–ICP-MS. In: Sylvester, P. J. (ed.) *Laser Ablation-ICP-Mass Spectrometry in the Earth Sciences: Principles and Applications*. Mineralogical Association of Canada (MAC) Short Course Series **29**, 29–46.

Lewis, P. C., Glen, R. A., Pratt, G. W. & Clarke, I. (1994). *Bega-Mallacoota 1:250 000 Geological Sheet SJ/55-4: Explanatory Notes*. Sydney, NSW: Geological Survey, pp. 148.

Marsh, B. D. (1988). Crystal capture, sorting, and retention in convecting magma. *Geological Society of America Bulletin* **100**, 1720–1737.

McBirney, A. R. & Hunter, R. H. (1995). The cumulate paradigm reconsidered. *Journal of Geology* **103**, 114–122.

McCulloch, M. T. & Chappell, B. W. (1982). Nd isotopic characteristics of S- and I-type granites. *Earth and Planetary Science Letters* **58**, 51–64.

Müntener, O., Kelemen, P. B. & Grove, T. L. (2001). The role of H_2O during crystallization of primitive arc magmas under uppermost mantle conditions and genesis of igneous pyroxenites: an experimental study. *Contributions to Mineralogy and Petrology* **141**, 643–658.

Paterson, B. A., Stephens, W. E., Rogers, G., Williams, I. S., Hinton, R. W. & Herd, D. A. (1992). The nature of zircon inheritence in two granite plutons. *Transactions of the Royal Society of Edinburgh* **83**, 459–471.

Petford, N., Cruden, A. R., McCaffery, K. J. W. & Vigneresse, J. L. (2000). Granite magma formation, transport and emplacement in the Earth's crust. *Nature* **408**, 669–673.

Potts, P. J. (1987). *A Handbook of Silicate Rock Analyses*. Glasgow: Blackie.

Reid, J. B. & Hamilton, M. A. (1987). Origin of Sierra Nevadan granite: evidence from small scale composite dikes. *Contributions to Mineralogy and Petrology* **96**, 441–454.

Richards, S. W. & Collins, W. J. (2004). Growth of wedge-shaped plutons at the base of active half grabens. *Transactions of the Royal Society of Edinburgh* **95**, 309–317.

Rollinson, H. (1993). *Using Geochemical Data: Evaluation, Presentation and Interpretation*. Harlow: Longman.

Simpson, C. J. (1986). Volcanic–plutonic associations within the Bindook Volcanic Complex, Goodmans Ford–Bullio area, New South Wales. *Australian Journal Earth Science* **33**, 475–489.

Sparks, R. S. J. & Marshall, L. A. (1986). Thermal and mechanical constraints on mixing between mafic and silicic magmas. *Journal of Volcanology and Geothermal Research* **29**, 99–124.

Wager, L. R. & Deer, W. A. (1939). Geological investigations in East Greenland, Part III. The Petrology of the Skaergaard Intrusion, Kangerdlugssuaq, East Greenland. *Meddelelser om Gronland* **105**, 1–352.

Wall, V. J., Clemens, J. D. & Clarke, D. B. (1987). Models for granitoid evolution and source compositions. *Journal of Geology* **95**, 731–749.

Watson, E. B. & Harrison, T. M. (1983). Zircon saturation re-visited: temperature and composition effects in a variety of crustal magma types. *Earth and Planetary Science Letters* **64**, 295–304.

White, A. J. R. & Chappell, B. W. (1977). Ultrametamorphism and granitoid genesis. *Tectonophysics* **43**, 7–22.

Wiebe, R. A. (1968). Plagioclase stratigraphy: a record of magmatic conditions and events in a granite stock. *American Journal of Science* **266**, 690–703.

Wiebe, R. A. (1973). Relations between coexisting basaltic and granitic magmas in a composite dike. *American Journal of Science* **273**, 130–151.

Wiebe, R. A. (1993). The Pleasant Bay layered gabbro-diorite, coastal Maine: ponding and crystallization of basaltic injections into a silicic magma chamber. *Journal of Petrology* **34**, 461–489.

Wiebe, R. A. (1996). Mafic–silicic layered intrusions: the role of basaltic injections on magmatic processes and the evolution of silicic magma chambers. *Transactions of the Royal Society of Edinburgh* **87**, 233–242.

Wiebe, R. A. & Collins, W. J. (1998). Depositional features and stratigraphic sections in granitic plutons: implications for the emplacement and crystallization of granitic magma chambers. *Journal of Structural Geology* **20**, 1273–1289.

Wiebe, R. A., Blair, K. D., Sabine, C. P. & Hawkins, D. P. (2002). Mafic injections, hybridization, and crystal accumulation in the Pyramid Peak Granite, California: implications for emplacement and construction of a granitic pluton. *Geological Society of America Bulletin* **114**, 909–920.

Williams, I. S. (1992). Some observations on the use of zircon U–Pb geochronology in the study of granitic rocks. *Transactions of the Royal Society of Edinburgh* **83**, 447–458.

Wyborn, D. & Chappell, B. W. (1986). The petrogenetic significance of chemically related plutonic and volcanic rock units. *Geological Magazine* **123**, 619–628.

Wyborn, D. & Owen, M. (1986). *Araluen, New South Wales, 1:100 000 geological map commentary*. Canberra, ACT: Bureau of Mineral Resources, 44 pp.

Wyborn, D., Chappell, B. W. & Johnston, R. W. (1981). Three S-type volcanic suites from the Lachlan Fold Belt, southeast Australia. *Journal of Geophysical Research* **86**, 10335–10348.

APPENDIX: LOCATION AND ROCK TYPE FOR SAMPLES IN TABLE 2

Sample	Pluton	Rock type	Australian Metric Grid
KSS-2A	Kameruka	granodiorite	749513.0 5931384.0
KSS-5C	Kameruka	granodiorite	742013.0 5931784.0
KSS-7A	Kameruka	granodiorite	739913.0 5933384.0
KSS-8B	Kameruka	granodiorite	738613.0 5931184.0
DB 2	Kameruka	granodiorite	726913.0 5957184.0
DB 4	Kameruka	granodiorite	737013.0 5965184.0
DB 6	Kameruka	granodiorite	727213.0 5995284.0
DB 8	Kameruka	granodiorite	727313.0 5994884.0
DB 11	Kameruka	tonalite	727613.0 5994784.0
DB 12	Kameruka	granodiorite	727613.0 5994784.0
DB 13	Kameruka	tonalite	727513.0 5994884.0
BH 26	Kameruka	granodiorite	731913.0 5951184.0
BH 27	Kameruka	granodiorite	731913.0 5951184.0
AB 139	Pericoe	monzogranite	729713.0 5989884.0
AB 207	Pericoe	monzogranite	727413.0 5984284.0
DB 1	Pericoe	monzogranite	726913.0 5957284.0
DB 9	Pericoe	monzogranite	727413.0 5994784.0
DB 18	Pericoe	monzogranite	728213.0 5984284.0
AB 335	Illawambra	monzogranite	748713.0 5973584.0
AB 336	Illawambra	monzogranite	743613.0 5975184.0
AB 337	Illawambra	monzogranite	751213.0 5973884.0
AB 338	Illawambra	monzogranite	750613.0 5974984.0
AB 339	Illawambra	monzogranite	746613.0 5972484.0
BH 24	Kameruka	monzogranite	731913.0 5951184.0
BH 1	Kameruka	monzogranite	731813.0 5952184.0
BH 7	Kameruka	monzogranite	731713.0 5953184.0
BH 12	Kameruka	monzogranite	731913.0 5951184.0
BH 25	Kameruka	monzogranite	726813.0 5957184.0